University Mohamed Khider of Biskra

Faculty of sciences and technology

Department of Metallurgical Engineering

MASTER DISSERTATION

Theme

Design and fabrication of mini-Spark plasma sintering for novel Materials

Student: Supervisor:

BEN MOHAMED ALI   BEN ZINE Haroune Rachid

Jury:

Dr.	MESSAOUDI Salim	MCB	University of Biskra	President
Dr.	LAMMEDI Fatima Zohra	MCB	University of Biskra	Examiner

Academic year: 2020 - 2021

Acknowledgments

I would like to express all my gratitude and my warmest thanks as well as my sincere gratitude to Dr. Ben Zine Haroun Rachid for proposing this subject to me and for making so much effort and time to direct this work.

TABLE OF CONTENT

Chapter 1: Bibliographic synthesis

1.1. Part one: Concepts about powder metallurgy

1.2. Part two: Spark plasma sintering

List of figures

CHAPTER 1: BIBLIOGRAPHIC SYNTHESIS

CHAPTER 2: METHODOL

Chapter 3: RESULTS AND DISCUSSION

List of tables

List of abbreviations

PM: Powder metallurgy.

CIP: Cold Isostatic Pressure.

HP: Hot Pressing.

HIP: Hot isostatic pressing.

SPS: Spark plasma sintering.

PECS: pulsed electric current sintering.

DC: direct current.

PDC: Pulsed direct current.

CHAPTER 1:
BIBLIOGRAPHIC SYNTHESIS

1.1. Part one: Concepts about powder metallurgy

1.1.1. Introduction:

Unlike conventional metallurgy processes, which always involve the solidification of a molten metal, powder metallurgy starts with a metal powder and uses a consolidation process by reaction between powder particles which results in the formation of a continuous and coherent solid [1].

Powder metallurgy (PM) is a set of technological processes allowing the production of components of predetermined shapes from powders (metallic, ceramic or composite) whose particle size and constitution are mastered. This method allows the production of precise parts difficult to obtain by other processes and without losing of materials [1].

1.1.2. Technologies of metal powder production

There are various technologies for mass metal powder production, one of the main requirements for using of metal powder in additive manufacturing and receiving reliable and repeatable results is a spherical particle's form. Some technologies allow to produce a spherical or near to spherical powder shape directly after synthesis of powder, whereas the other technologies require a further processing to achieve the desired particles shape. Technologies for the production of metal powder conventionally are separated on base of the following methods:

- chemical methods.
- Physical methods.
- mechanical methods.

The physical and chemical methods are associated with physical and chemical transformations, chemical composition, and structure of the final product (metal powder) and significantly differ from raw materials. The mechanical methods include various types of milling processes and jet dispersion melts by high pressure of gas or liquid (also known as atomization) [2].

1.1.3. Powder metallurgy Processes

There are several methods of forming bits of powder stock. Many of these manufacturing processes have characteristics similar to their conventional powder processing technology. Processing similarities will depend on similar reactions and mechanisms within the material.

Although some factors are similar, powder processes will have differences in their methods. Differences in the manufacturing process will affect the size, geometry and complexity of the portion that can be produced. Some special powder processes may be well suited to a specific type of part. The mechanical properties of the product material will also depend on the type of energy mining process used [3].

1.1.3.1. Isostatic Pressing

Isostatic pressing is similar to uniaxial pressing in the requirements for the powder and in the general steps of the process, but there are several important differences. First, the compaction takes place under hydrostatic conditions. That is, the pressure is transmitted to the part equally in all directions, or very nearly equally. In this way, the die wall friction is significantly reduced or eliminated entirely. Second, the tooling consists of elastomeric molds rather than rigid dies. The powder is loaded into the flexible mold, the mold is sealed and the pressure is applied in a pressure vessel via a liquid [3].
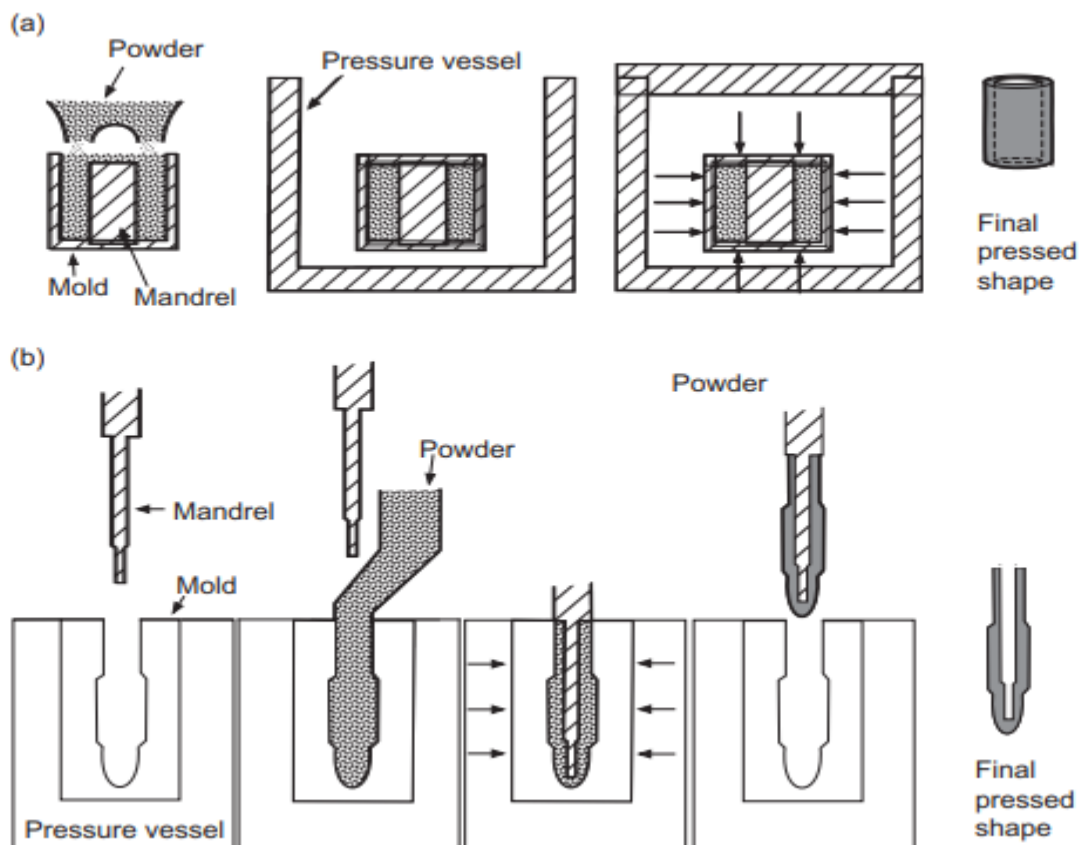
FIGURE 1.1.1. Schematic diagrams for (a) wet bag isostatic pressing with collapsing bag tooling, including a mandrel, to make a tube and (b) dry bag isostatic pressing [4].

1.1.3.2. Cold Isostatic Pressing

Cold isostatic pressing consists in compacting a dry or semi-dry powder in an elastomeric mold submersed in a pressurized liquid. Rigid tooling (e.g., a steel mandrel) is often combined with the flexible elastomeric mold to ease shaping. Typical forming pressures for ceramics are in the 20–200 MPa range [5].
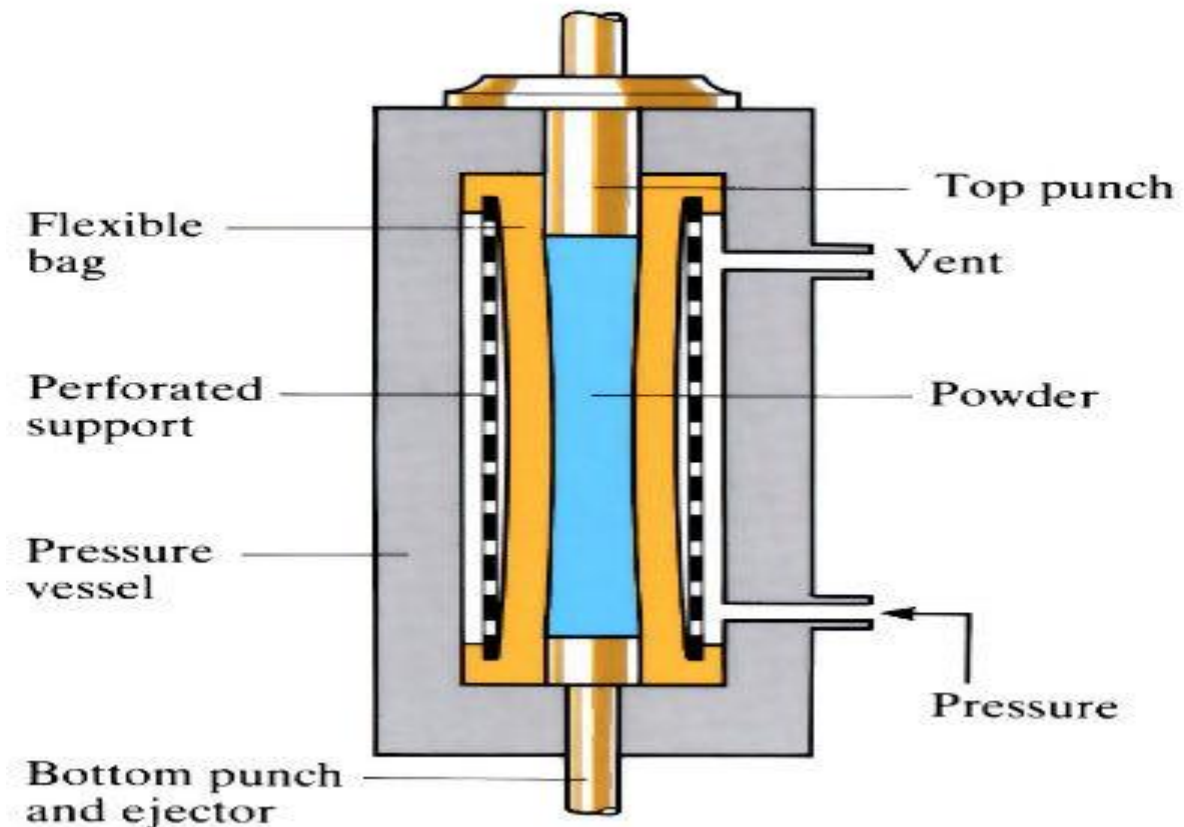
Figure 1.1.2. Principle of Cold Isostatic Pressing (CIP) [6].

1.1.3.3. Roll Compaction

Roll compaction is a continuous manufacturing process aiming to produce particulate granules from powders. A Roll press typically consists of a screw feeding system, two rolls and a side sealing. Despite its conceptual simplicity, numerical modelling of the process is challenging due to the complexity involving two different mechanisms: feeding by the screw and powder compaction between the rolls [7].
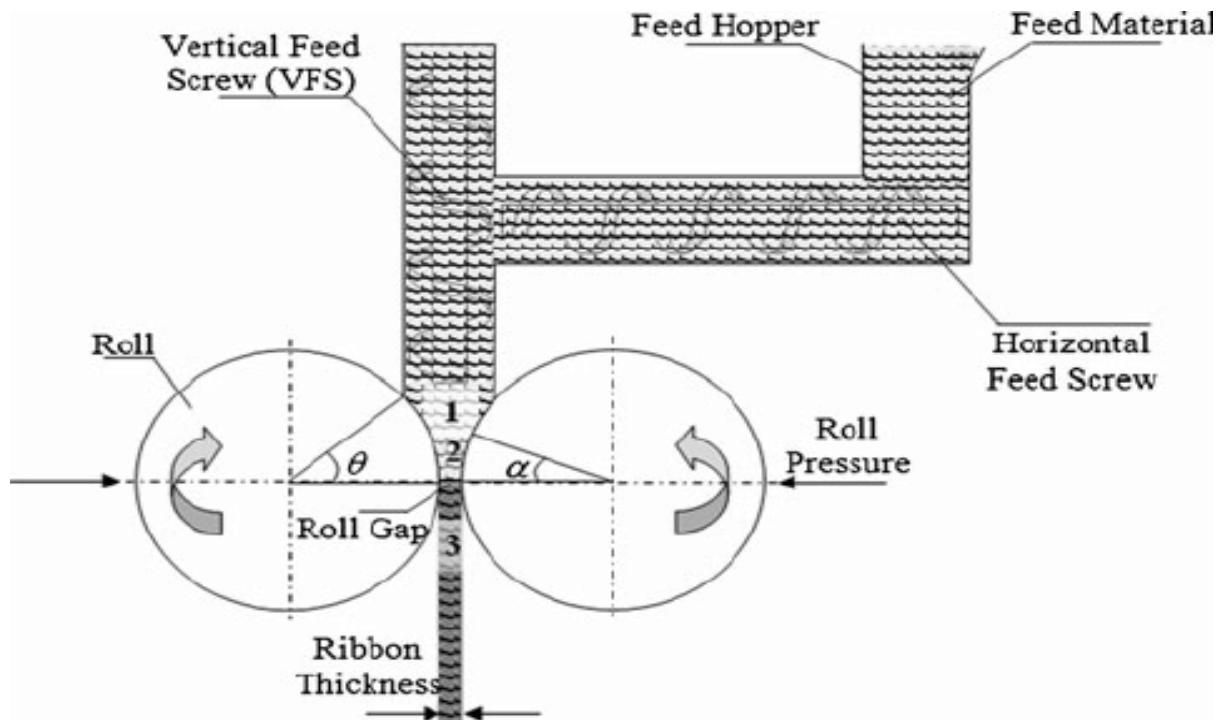
Figure 1.1.3. Schematic diagram of the roller compaction process [8].

1.1.3.4. Hot Pressing

Hot pressing is performed in a rigid die using loading along the vertical axis. To avoid die damage, the graphite die is enclosed in a protective atmosphere or vacuum chamber. Loading is along the vertical axis on punches pressurized from an external hydraulic system. Although the pressure is applied along the vertical axis, there is a radial pressure against the die wall. The differential stress between the axial and radial directions generates shear that is effective in particle bonding. This shear stress is proportional to the applied stress. Initial densification includes particle rearrangement and plastic flow. As densification progresses, creep by grain boundary diffusion and volume diffusion becomes controlling [9].
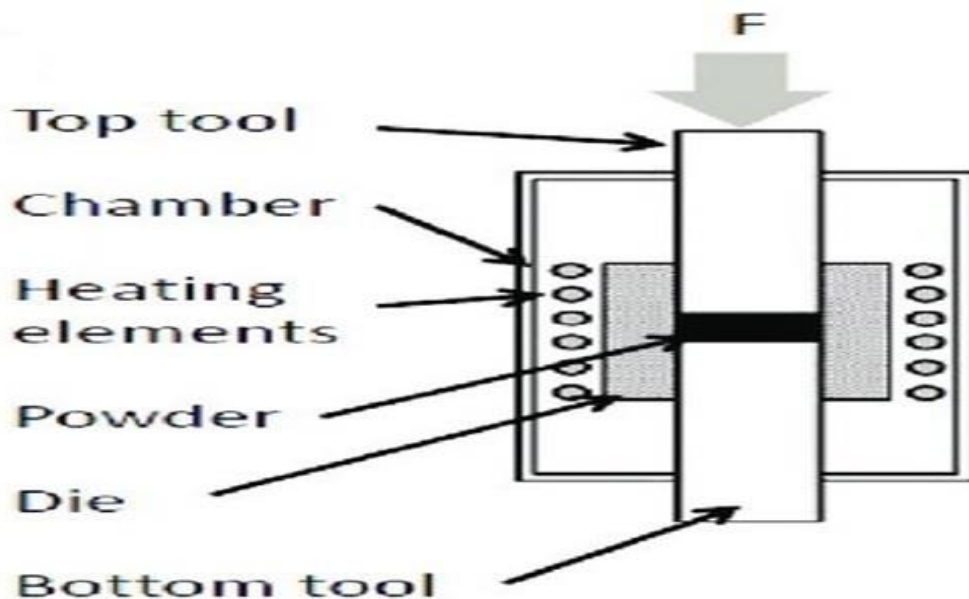
Figure 1.1.4. Principle of hot pressing (HP) [10].

1.1.3.5. Hot Isostatic Pressing

Hot isostatic pressing, (HIP) is a pressure enhanced sintering technique. This technique is used to manufacture dense products. For isostatic compaction the powders must be encapsulated in an evacuated gas-tight welded can. The can transfers the pressure to the powders. This can or mold can be mild steel, stainless, a metal, or a glass capsule. The HIP process subjects powders to simultaneous elevated temperatures of over 1000 °C and pressures of over 98 MPa to eliminate internal micro-shrinkage [11].
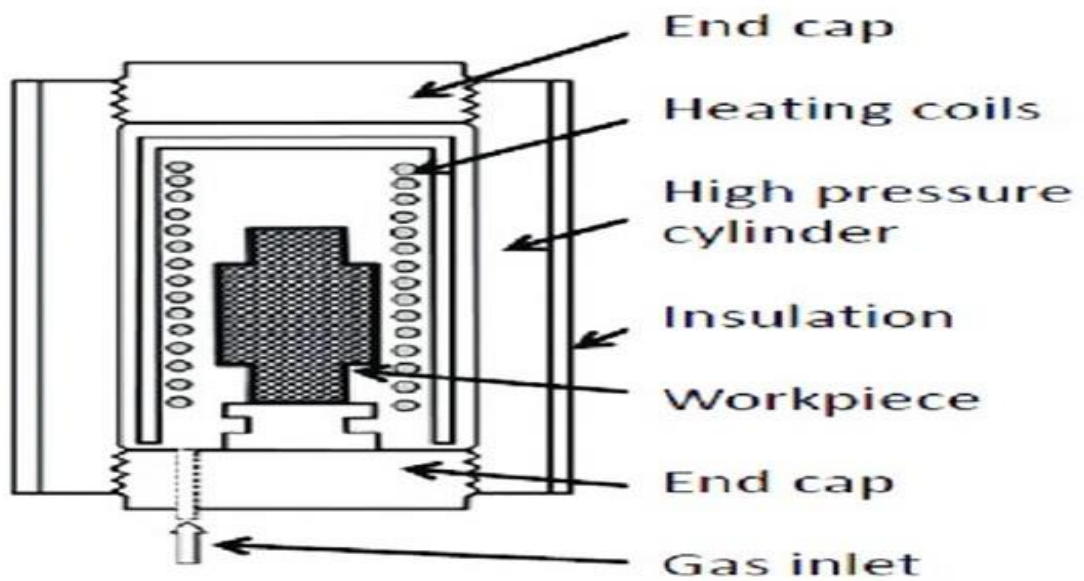
Figure 1.1.5. Schematic diagram of hot Isostatic pressing (HIP).[10]

1.1.3.6. Powder Extrusion

Powder extrusion is a powder metallurgy process used to manufacture parts with high length to diameter ratios. In this manufacturing process, powders are placed in a container of thin sheet metal. This is evacuated and sealed, producing a vacuum inside. The container containing the powder is then extruded [12].
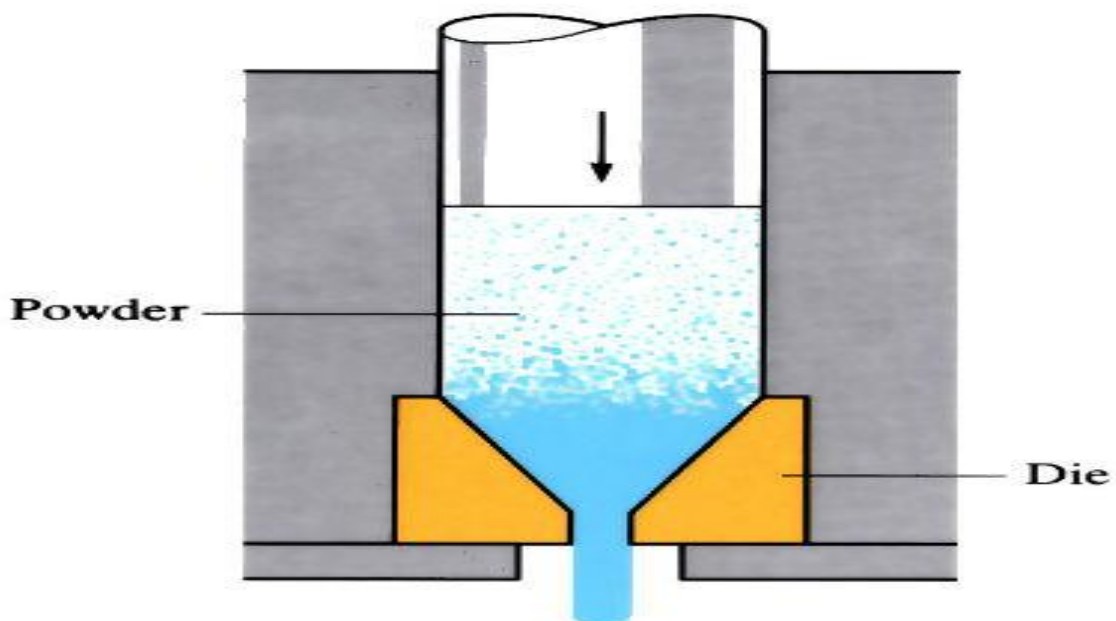
Figure 1.1.6. Schematic diagram of Powder Extrusion [13].

1.1.3.7. Spark plasma Sintering

Spark plasma sintering (SPS) is a rapid technique. Its processing parameters are usually low-voltage and low-pressure acting, using a uniaxial force and pulsed direct current (DC) to carry out high efficiency consolidation of the powder. This technique has been widely applied for various materials processing in the recent years [14]. SPS closely resembles hot-pressing (HP), but differs from the latter in the heating source [15].
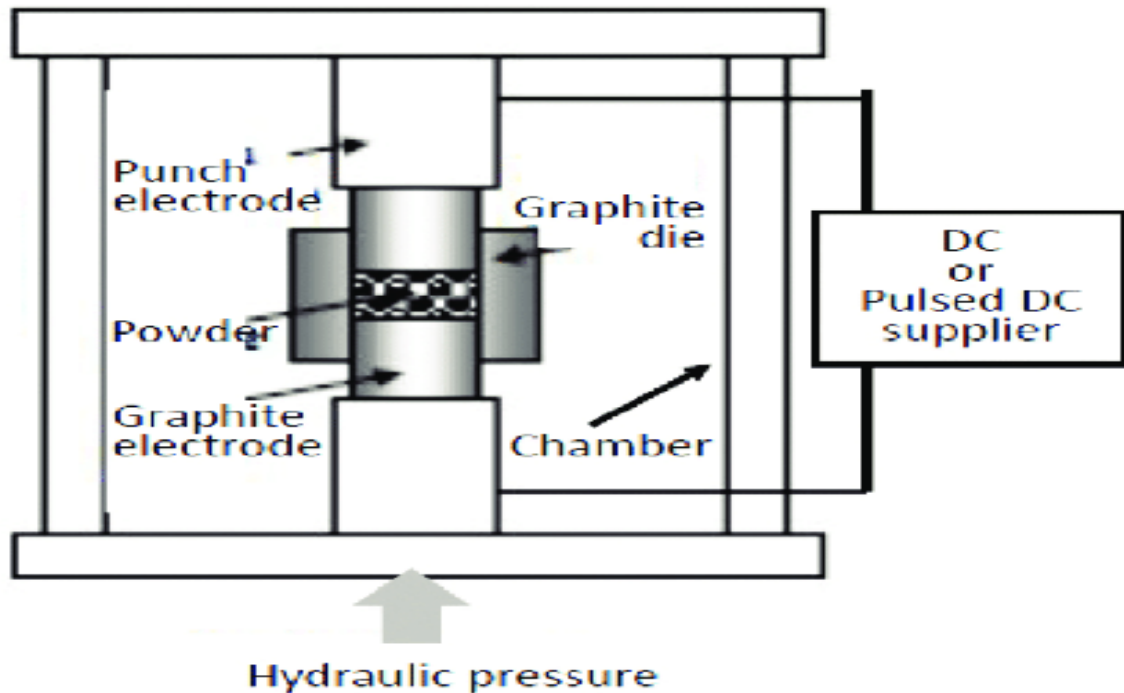
Figure 1.1.7. Principle of Spark plasma Sintering [10].

1.1.3.8. Metal Injection Molding

Metal injection molding is a manufacturing method that combines traditional PM with plastic injection molding. Over the past decade it has established itself as a competitive manufacturing process for small precision components that would be costly to produce by alternative methods. It can be used to produce comparatively small parts with complex shapes from almost any type of material such as metals, ceramics, inter-metallic compounds [16].
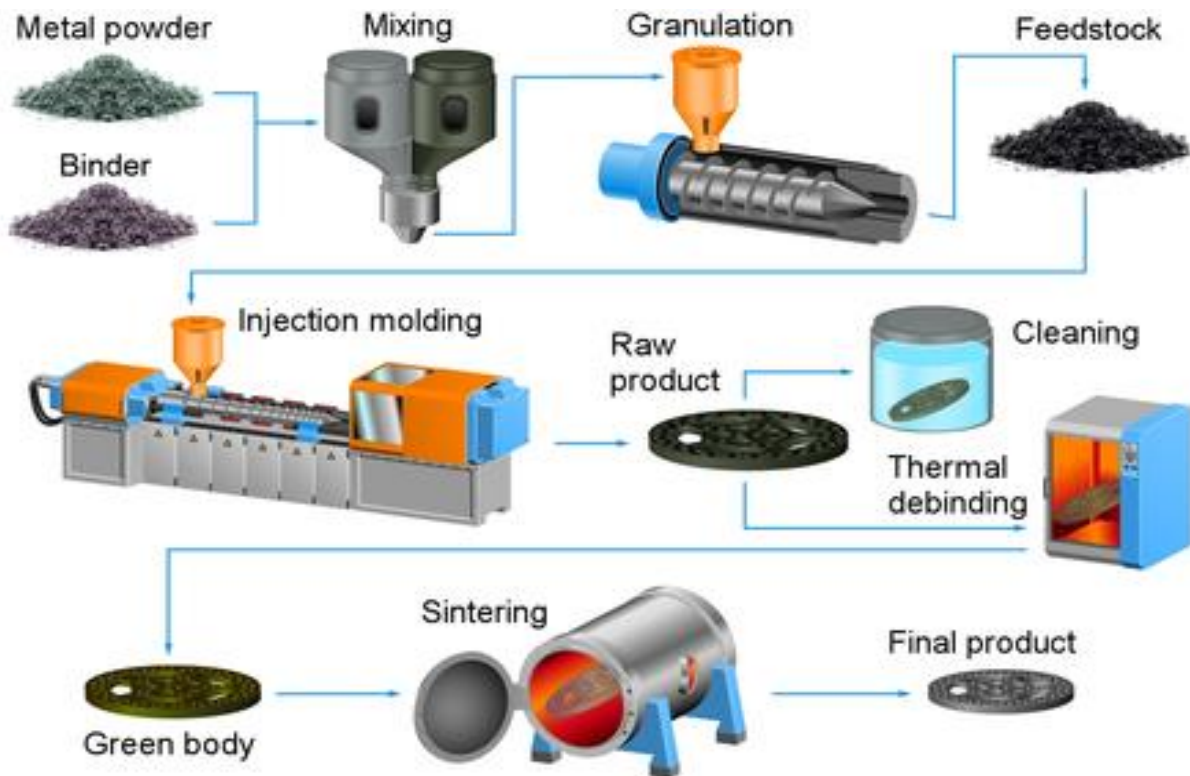
Figure 1.1.8. Schematic diagram of Metal Injection Molding [17].

1.2. Part two: Spark plasma sintering

1.2.1. Introduction

The term Spark Plasma Sintering (SPS) is generally used to identify a sintering technique involving the simultaneous use of uniaxial pressure and high-intensity, low-voltage, pulsed current. In general terms, SPS can be considered a modification of hot pressing, where the furnace is replaced by the mold containing the sample, that is heated by a current flowing directly through it and eventually through the sample. However, since there is no general agreement on the details of the technique, an unequivocal definition of the SPS and its associated procedures cannot be defined [18,19]. The name SPS itself has been often disputed as, despite several attempts, the presence of plasma and electric discharges during the process it has never been proved unequivocally [19].

SPS has been receiving growing attention in the last two decades due to its remarkable effectiveness, allowing to obtain fast sintering and densification, particularly in the case of materials considered hard to sinter, such as extremely refractory materials, metastable phases or nanomaterials. For some of these materials, SPS has already become the sintering technique of choice [20,21].

SPS belongs to a quite extensive group of techniques involving the use of electric current for the sintering of materials. Some of these techniques have been introduced, and found widespread application, since the beginning of the last century, particularly for metallic materials [22,23]. The most distinctive characteristics of SPS, represented by the use of pulsed DC, appeared originally in a patent by Inoue in the mid '60 of the last century, while the term SPS was introduced later on, by the Japanese producers of the first commercial machines. In the beginning, the technique found application mostly in Japan and in a few other far-east countries. The diffusion in western countries, mainly in research institutions, started in the mid '90 of the last century and spread rapidly in the industrial environment [23].

1.2.2. Definition

Spark plasma sintering (SPS) or pulsed electric current sintering (PECS) is a sintering technique utilizing uniaxial force and a pulsed (on-off) direct electrical current (DC) under low atmospheric pressure to perform high speed consolidation of the powder. This direct way of heating allows the application of very high heating and cooling rates, enhancing densification over grain growth promoting diffusion mechanisms (see Fig.1.2.1), allowing maintaining the intrinsic properties of Nano powders in their fully dense products [24].
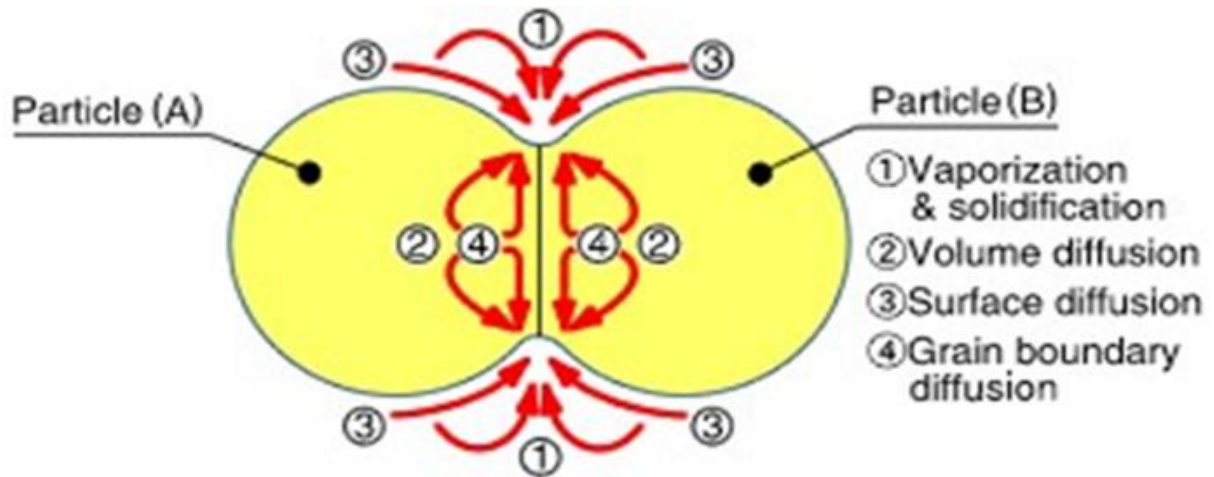
Figure 1.2.1. Material transfer path during sintering [24].

It is regarded as a rapid sintering method in which the heating power is not only distributed over the volume of the powder compact homogeneously in a macroscopic scale, but moreover the heating power is dissipated exactly at the locations in the microscopic scale, where energy is required for the sintering process, namely at the contact points of the powder particles (see Fig.1.2. 2). This fact results in a favorable sintering behavior with less grain growth and suppressed powder decomposition. Depending on the type of the powder, additional advantageous effects at the contact points are assumed by a couple of authors.[24]
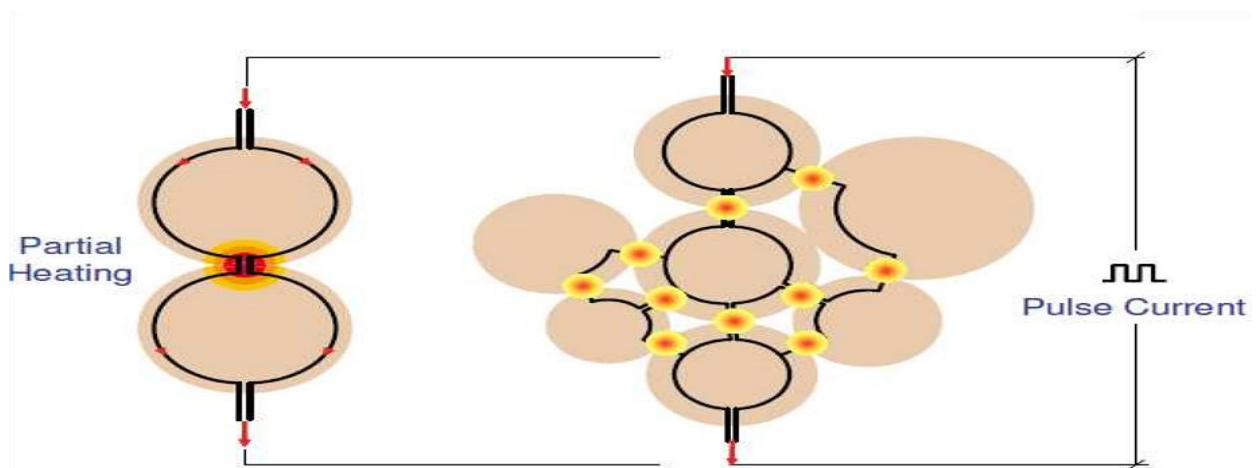
Figure.1.2.2. Energy dissipation in the microscopic scale [24].

1.2.3. Configuration of sps process

The basic configuration of a typical SPS system is shown in Figure.1.2.3. The system consists of a SPS sintering machine with vertical single-axis pressurization and built-in water-cooled special energizing mechanism, a water-cooled vacuum chamber, atmosphere controls, vacuum exhaust unit, special sintering DC pulse generator and a SPS controller. The powder materials are stacked between the die and punch on the sintering stage in the chamber and held between the electrodes. Under pressure and pulse energized, the temperature quickly rises to 1000~2500 °C above the ambient temperature, resulting in the production of a high-quality sintered compact in only a few minutes [24].
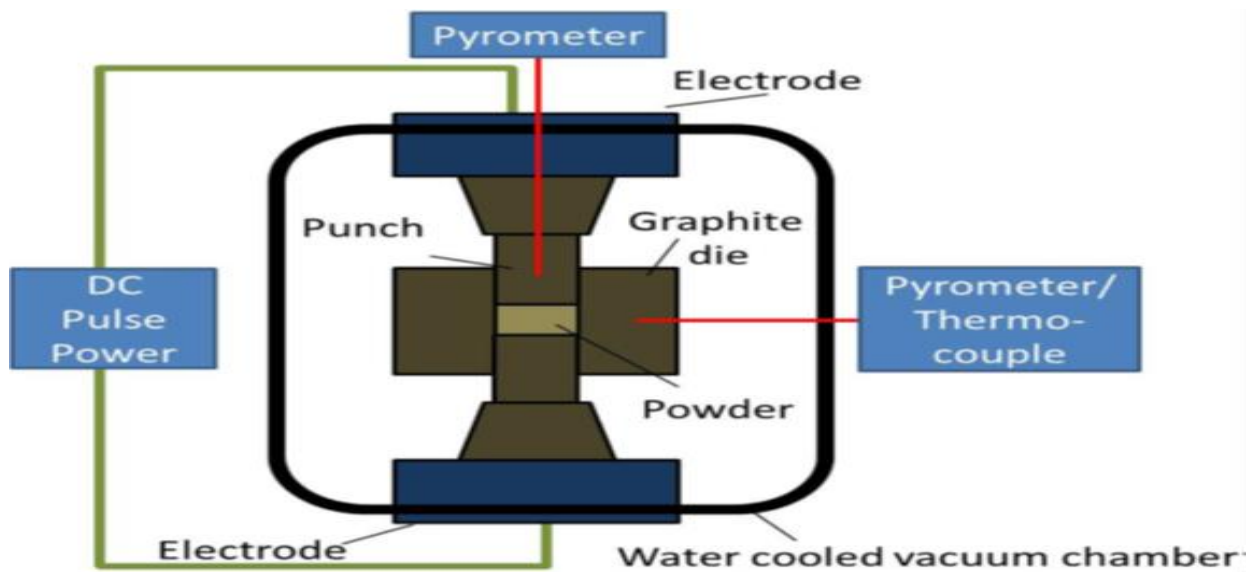
Figure.1.2.3. SPS system configuration.[24].

1.2.4. Principles and mechanism of the SPS process

The SPS process is based on the electrical spark discharge phenomenon: a high energy, low voltage spark pulse current momentarily generates spark plasma at high localized temperatures, from several to ten thousand °C between the particles resulting in optimum thermal and electrolytic diffusion. SPS sintering temperatures range from low to over 2000 °C, which are 200 to 500 °C lower than with conventional sintering. Vaporization, melting and sintering are completed in short periods of approximately 5 to 20 minutes, including temperature rise and holding times [25]. Unique to SPS process is the mechanism of internal heat generation due to DC as opposed to the other conventional methods of sintering, such as hot pressing, where external heat is supplied to the sample. Conventional sintering processes could require hours, whereas SPS would take only a few minutes to achieve the

same or better consolidation [26]. It combines the compaction and sintering stages into a single operation. The mechanical scheme of the process is very similar to the uniaxial die pressing. The load applied during SPS is transferred to the sample through the upper punch. The pulsed DC power supply is connected to the upper and lower punches/electrodes. The SPS process is a highly energy-efficient process and is easy to operate. It can be used to process conductive as well as non-conductive materials to attain very high levels of densification. SPS provides uniform sintering and also low grain growth which is why it is an ideal process for processing nanostructured materials [27,28]. Several explanations have been proposed for the effect of SPS:

1.2.4.1. Plasma generation

The inventors of the SPS process originally claimed that pulsed generate sparks and even plasma discharges between particle contacts, which were the reason for naming the processes, plasma spark sintering and activated plasma sintering [29,30]. They claim that the ionization on contact with the particles due to spark discharges has developed "impulsive pressures" that facilitate the diffusion of the atoms upon contact [31]. It has been suggested that the pulsed current has a cleaning effect on particle surfaces based on the observation of grain boundaries without oxidation forming between the particles. Whether plasma is generated or not has not been directly confirmed by experiments. Therefore, there is no conclusive evidence for the effect of plasma generation in SPS. The occurrence of plasma discharge is still a matter of debate, but it appears to be widely accepted that accidental electrical discharges may occur at a microscopic level [32].

1.2.4.2. Joule heating

Joule heating due to the passage of electric current through particles assists in the welding of the particles under mechanical pressure. The intense joule heating effect at the particle conducting surface can often result in reaching the boiling point and therefore leads to localized vaporization or cleaning of powder surfaces. Such phenomenon ensures favorable path for current flow [33]. A volume heating resulting from the Joule effect in contrast to the conductive heat transport that takes place during conventional sintering enables a rapid rise in the temperature which in turn enhances the mass transport mechanisms responsible for the sintering phenomenon. The intense Joule heating effect at the particle surface can often be very high, and the boiling point of the particle could be attained and thereby lead to localized vaporization or cleaning of the powder surfaces. This, in turn, improves the consolidation rate. In processes like hot pressing, the die and the sample are heated by radiation from

an enclosing furnace. The pulsed DC also creates plasma, which causes a cleaning effect on the surface of the particles leading to sintering enhancement. In order to achieve a homogeneous sintering behavior, the temperature gradients inside the sample should be minimized. Adequate electrical conductivity of the powder samples and the achievement of homogeneous temperature distribution during sintering is a major concern of the SPS process. The important parameters which influence the temperature gradient within the sample are electrical conductivity of the materials constituting the sample, the pulsed current input and the wall thickness of the die [34].

Graphite papers are used to avoid direct contact between the graphite parts and the sample and also to guarantee electrical contact between all parts. Figure.1.2.4 shows the mechanism of Joule heating during SPS.
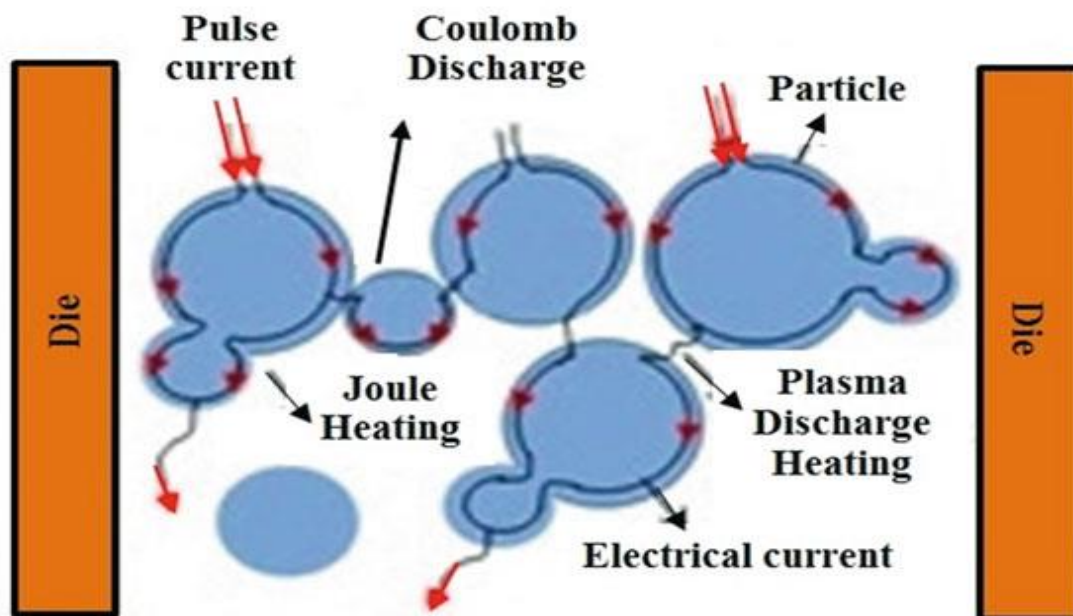
Figure.1.2.4. Joule heating during SPS [34].

1.2.4.3. Pulsed current

The ON-OFF DC pulse energizing method generates: (1) spark plasma, (2) spark impact pressure, (3) Joule heating, and (4) an electrical field diffusion effect (see figure.1.2.5).
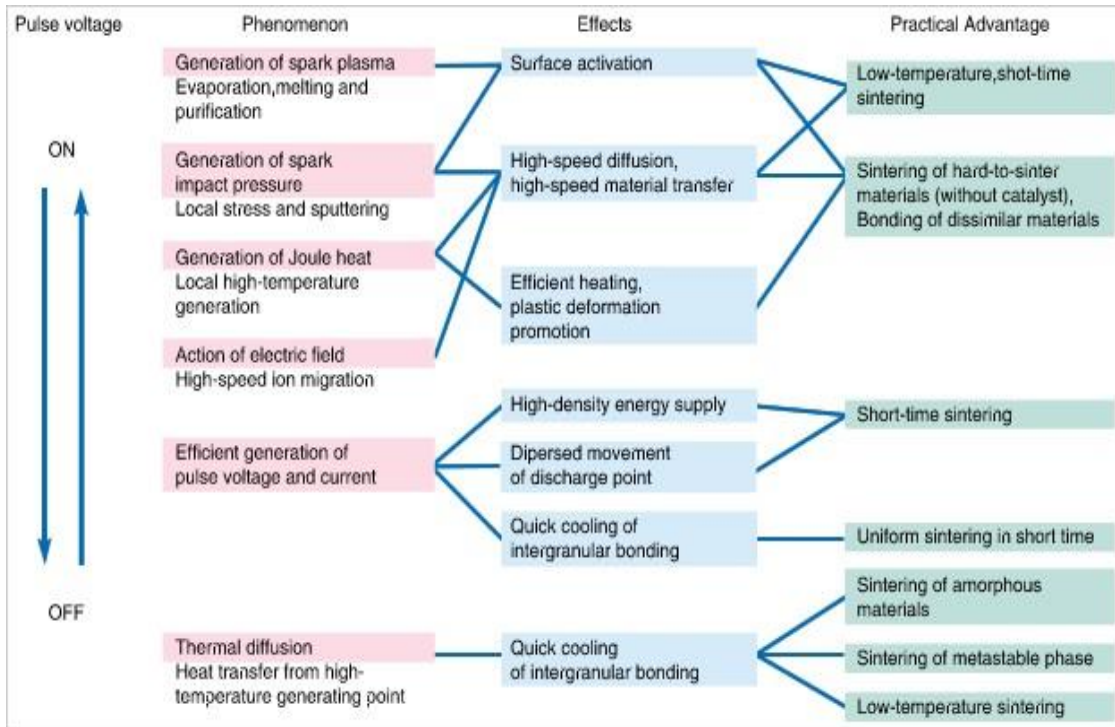
Figure.1.2.5. Effects of ON-OFF DC [34].

When a spark discharge appears in a gap or at the contact point between the particles of a material, a local high-temperature state (discharge column) of several to ~10,000 °C is generated momentarily. This causes evaporation and melting on the surface of the powder particles, and necks are formed around the area of contact between the particles. Figure.1.2.6 shows the basic mechanism of neck formation during SPS. The heat is transferred immediately from the center of the spark discharge column to the sphere surface and diffused so that the intergranular bonding portion is quickly cooled. The pulse energizing method causes spark discharges one after another between the particles. In a single particle itself, the number of positions where necks are formed between the adjacent particles increases as the discharges are repeated [35].
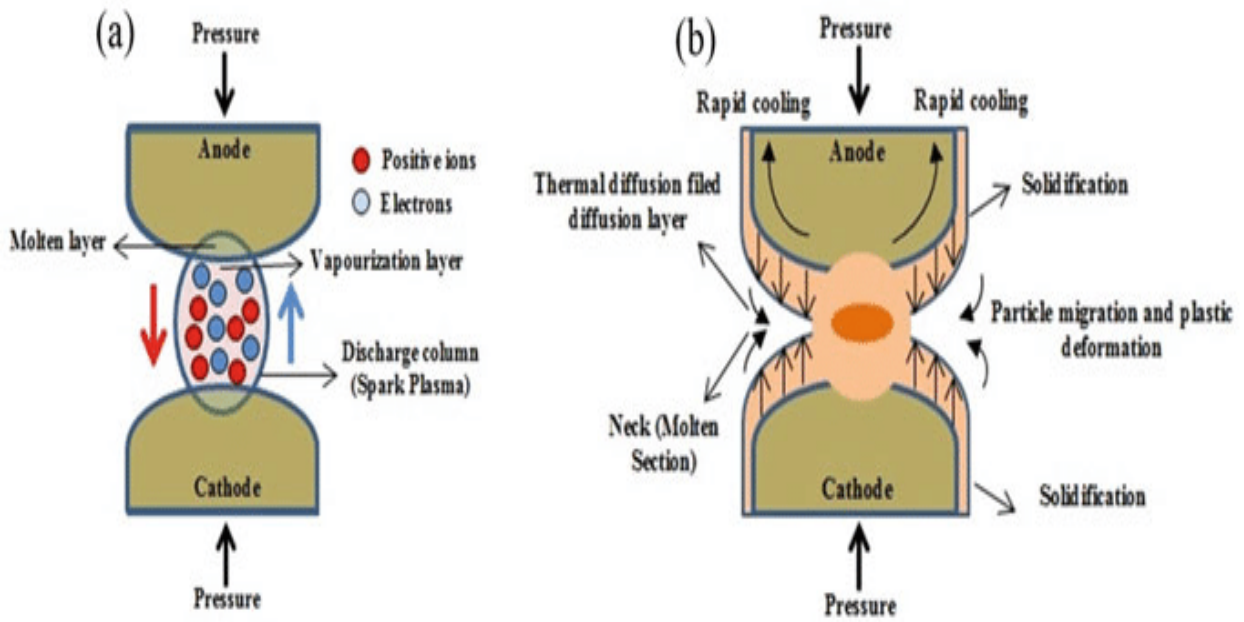
Figure.1.2.6. (a) Vaporization and melting on particle surface, (b) neck growth in the presence of spark plasma [35]

The SPS process is an electrical sintering technique which applies an ON-OFF DC pulse voltage and current from a special pulse generator to a powder of particles (see figure.1.2.7), and in addition to the factors promoting sintering, also effectively discharges between particles of powder occurring at the initial stage of the pulse energizing for sintering [35].
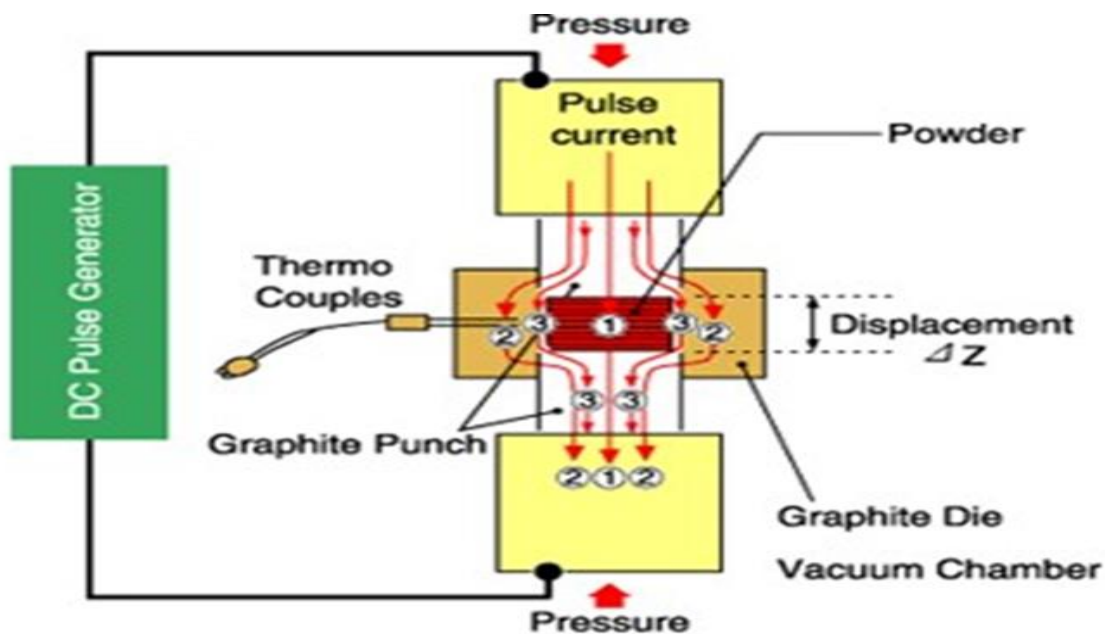
Figure.1.2.7. ON-OFF pulsed current path through the spark plasma sintering machine [35].

High temperature sputtering phenomenon generated by spark plasma and spark impact pressure eliminates adsorptive gas and impurities existing on the surface of the powder particles. The action of the electrical field causes high-speed diffusion due to the high-speed migration of ions [35].

1.2.4.4. Mechanical pressure

Typically, the maximum loading pressure during SPS lies in the range of 80–140 MPa. Due to the simultaneous application of pressure and temperature during SPS, almost complete densification can be achieved at a sintering temperature which is lowered by 200–250 °C as compared to other conventional sintering processes. In the conventional sintering process, usually, a green compact is initially prepared externally using a suitable die and punch by the application of necessary pressure via hydraulic machine. On the other hand, along with the high DC pulse which is passed between the graphite electrodes an axial pressure is simultaneously applied right from the beginning of the sintering cycle in SPS. The actual contact area between the particles depends on the contact pressure and is usually only a small fraction of the apparent contact area. During the SPS process, imperfect contacts caused by surface roughness, impurities, insulating layers or oxides lead to complex and unpredictable thermal and electrical behavior at the interfaces. The contact resistance is a function of the actual area of contact, electrical resistivity and interface temperature. A SPS-sintered grain boundary undergoes plastic deformation after the completion of sintering. The heated material becomes softer, and it undergoes plastic deformation under the uniaxial load. The SPS process is thus a combination of three stages. Plasma heating is the first stage of SPS. During this stage, the electrical discharge between the particles results in localized and momentary heating of the particles to several thousands of degrees. As the micro-plasma discharge forms throughout the volume of the sample, heat is generated uniformly. At high temperatures, the impurities concentrated on the particle surfaces are vaporized, and the surface of the particles is purified and activated. The purified surface layers of the particles then melt and fuse with each other forming necks between them. At this stage, the pulsed DC electrical current flows from the particles through the necks connecting them. The Joule heat generated by the electrical current increases the diffusion of atoms in the neck, enhancing their growth. The localized character of heating and its uniform distribution allows rapid temperature rise and drop which diminishes grain coarsening. Finally, the heated material becomes soft, and it undergoes plastic deformation under the uniaxial load which is applied during the sintering process [36]. During SPS plastic deformation combined with diffusion results in densification of the powder compact to above 99% of its theoretical density [36].

1.2.5. Advantages and Disadvantages of spark plasma sintering

The term SPS includes a convenient description of the process as it enables sintering, adhesion, crystal growth, and chemical reactions [22]. Compared with traditional sintering processes, SPS has many features that can provide a wide range of possibilities for developing new materials.

1.2.5.1. Advantages of plasma spark sintering [37]

- ❖ Fast and uniform sintering.
- ❖ Low grain growth (ultrafine grain materials can be prepared).
- ❖ The phases of compression and sintering are combined in one operation.
- ❖ Better purification and revitalization of powder particle surfaces.
- ❖ Can process different materials (metals, ceramics, compounds).
- ❖ Generating the temperature gradient during sintering which allows sintering of functionally graded materials.
- ❖ Solid state sintering.
- ❖ Sintering at low temperatures.
- ❖ The possibility of influencing the sintered material by the energy of the electromagnetic field.

1.2.5.2. Disadvantages of plasma spark sintering [37]

- ❖ Only simple symmetric shapes can be prepared.
- ❖ An expensive DC pulse generator is required.

1.3. Part three: Relative Electrical parameters and notions.

1.3.1. Electric tension

Electric voltage is the flow of the electric field along an electric circuit measured in volts by a voltmeter. It is denoted V across a dipole [38].

More generally, the existence of a voltage in an electrical circuit made up of elements of non-zero resistance, is proof of the existence in this circuit of an electric generator maintaining a voltage at its terminals [38].

1.3.2. Direct current (DC)

Direct current (DC) is the one directional flow of electric charge. An electrochemical cell is a prime example of DC power. Direct current may flow through a conductor such as a wire, but can also flow through semiconductors, insulators, or even through a vacuum as in electron or ion beams. The electric current flows in a constant direction, distinguishing it from alternating current (AC) [39].

The abbreviations AC and DC are often used to mean simply alternating and direct, as when they modify current or voltage [40].

Direct current has many uses, from the charging of batteries to large power supplies for electronic systems, motors, and more. Very large quantities of electrical energy provided via direct-current are used in smelting of aluminum and other electrochemical processes. High-voltage direct current is used to transmit large amounts of power from remote generation sites or to interconnect alternating current power grids [40].

1.3.3. Pulsed direct current (PDC)

An alternating current is changed into a pulsating direct current after having been rectified by the rectifier circuit. Between the electrodes a varying high voltage is maintained by a pulsating direct current supplied thereto. A pulsating DC current is applied to the anode and the cathode. This type of current can be used for plasma generation purposes. Plasma generated using PDC is more reliable than that created by regular direct current, as it cannot be poisoned by the build-up of argon gas [41].

1.3.4. Pulsed direct current generator

A direct-current (DC) generator is a rotating machine that supplies an electrical output with unidirectional voltage and current. The basic principles of operation are the same as those for synchronous generators. Voltage is induced in coils by the rate of change of the magnetic field through the coils as the machine rotates. This induced voltage is inherently alternating in form since the coil flux increases and then decreases, with a zero-average value [41].

Figure.1.3.1. 20kW Pulsed DC Plasma Generator [41].

CHAPTER 2:
METHODOLOGY

2.1. Objective

In this chapter, we will show the different setups used to investigate the thermal and electrical properties of graphite and sintering process.

2.2. Experimental setup

Figure 2.1. is a schematic representation of the experimental setup, figure 2.2 shows the experimental setup. A graphite rod is directly connected to the DC generator. A timer and an infrared thermometer are used to measure the time and temperature, respectively. The DC intensity is controlled from the generator as shown in figure 2.3.
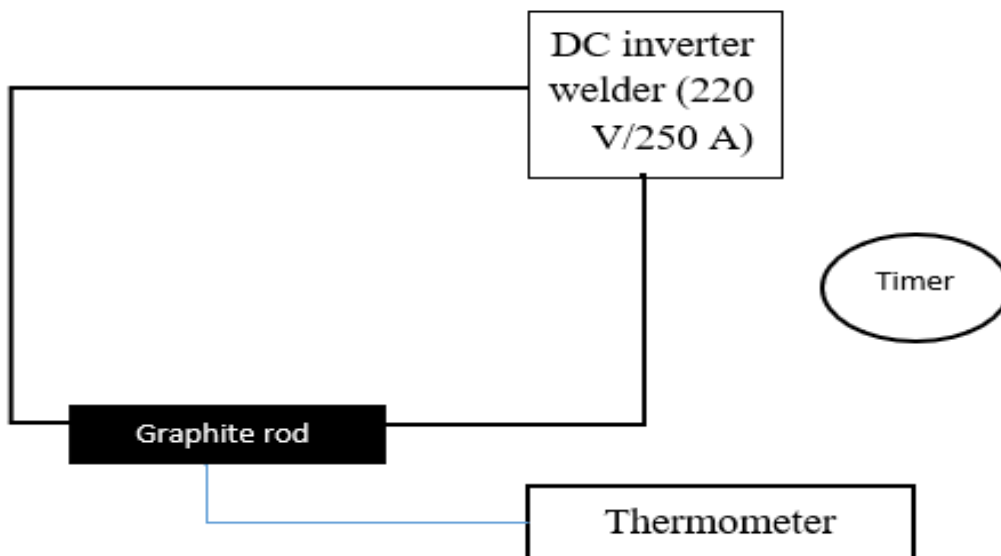
Figure 2.1. schematic representation of the experimental setup.

Figure 2.2. The experimental setup.

Figure 2.3. Generator controller.

2.3. Equipment

The equipment used in the experiment for measuring graphite properties are (Figure 2.4):

- 220 V/250 DC inverter welder (a).
- Thermometer (b).
- Multimeter (c).
- timer (d).

Figure 2.4. The apparatus used in the experiment, a): 220 V/250 DC inverter welder, b): Thermometer, c): Multimeter, d): timer.

- for security reasons we made the box in Figure 2.5, the box is made using a wooden base, an iron fence, iron frame, and ceramic base to protect the user during the experiment from any unexpected explosion that may result from electrical overload or excessive heat.
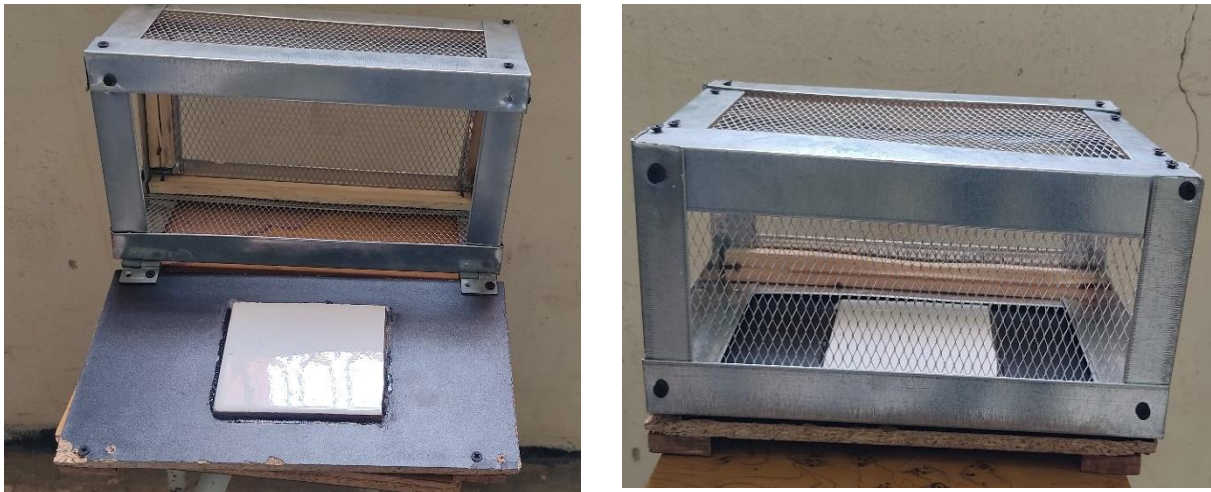
Figure 2.5. (a): open box, (b): Closed box.

- The Multimeter is used to measure the electrical conductivity of graphite as shown in figure 2.6.

Figure 2.6. Measurement of the electrical conductivity of graphite by multimeter.

- Figure 2.7. shows the Connect of a graphite to Dc generator.
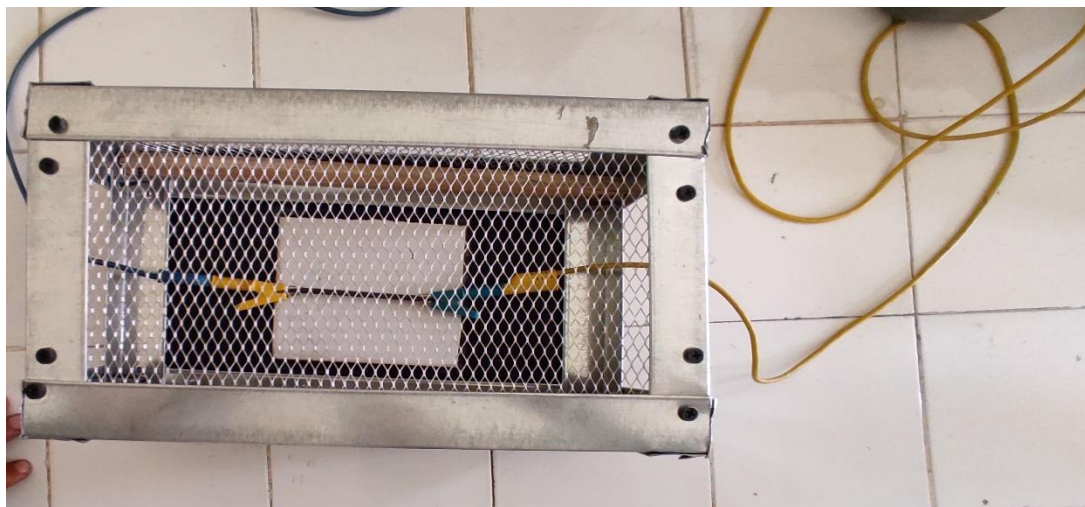
Figure 2.7. Connect the graphite to a generator.

- The infra-red thermometer is used to measure the graphite temperature during the experiment as shown in figure 2.8.

Figure 2.8. Graphite temperature measurement by Thermometer .

2.4. Materials

The substance used is graphite, which is a type of mineral, 99.9% synthetic graphite is made in electric furnaces using petroleum coke. It is used to make electrodes and brushes for electric motors. In our experiment we used different types of graphite available in the market and from used batteries as shown in figure 2.9.

Figure 2.9. Graphite rod, a): sample 1, b): sample 2, c): sample 3.

As shown in Table 2.1, we used three types of metal powders in our experiment.
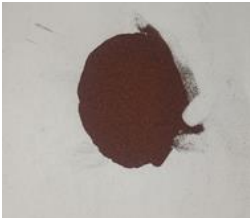
Metal powders	Particle size distribution	Chemical composition
Iron powder	106 μm …………≤ 1 % 75 μm ……….0 - 10 % 45 μm………15 – 65 %	Fe... ... ...…. ... .≥ 95% Carbon... ... .… ... .≤ 0.06%
Copper powder		Fe... ... ... ≤ 0.02% Chloride (Cu)...…. ≤ 0.04% Ag... ... ...… ... ...…. ≤ 0.005% Moisture... ... ...…. ≤ 0.05
Aluminum powder		Iron (Fe)... ....≤ 0.5 % lead (Pd)..... ≤ 0.03 % Arsenic (As).. ≤ 0.0005 %

Table 2.1. Metals powder chemical characteristics

CHAPTER 3:
RESULTS AND DISCUSSION

3.1. Introduction

In this chapter, we will discuss our results after investigating the thermal and electrical properties of graphite.

After measuring the resistivity and dimensions of the different types of graphite used in our experiment, the measured resistivity for sample 1, sample 2, sample 3, is (1.9 Ω, 1.5 Ω, 6.7 Ω) respectively as shown in table 3.1.

Table 3.1 shows the dimensions and the resistivity of the different types of graphite.

Graphite rod	Simple 1	Simple 2	Simple 3
Resistivity (Ω)	1.9 (Ω)	1.5 (Ω)	6.7 (Ω)
Diameter (mm)	8 (mm)	4 (mm)	a=b=0.6 (mm)
Length (mm)	56 (mm)	47 (mm)	65 (mm)

Table 3.1: The dimensions and the resistivity of the different types of graphite.

3.2. Investigation of graphite samples properties

3.2.1. Sample 1

As shown in table 3.2, we measured the graphite temperature change for 6 minutes using 30 s intervals at 25 A, 50 A, 75 A, 100 A, 150 A and 200 A. We can clearly observe the increase of the temperature with the increase of the time and current density.

At 100 A, the graphite sample exceeded the thermometer temperature limit after 300 s. The same thing was observed at 150 A after 180 s, and for 200 A after 90 s.

Time (s)	25 A	50 A	75 A	100 A	150 A	200 A
30	50	106	120	189	250	652
60	67	130	170	248	363	755
90	84	141	200	303	513	900
120	90	165	220	398	628	/
150	95	191	282	428	758	/
180	100	205	350	643	900	/
210	104	226	421	717	/	/
240	111	251	430	725	/	/
270	125	261	463	760	/	/
300	131	274	490	900	/	/
330	141	280	570	/	/	/
360	151	300	600	/	/	/

Table 3.2. representation of the data (sample 1).

Figure 3.1 shows the heated graphite (sample 1) during our experiment at different current densities, the higher increase in graphite brightness is related to the increase in graphite temperature.

Figure 3.3.1: heated graphite (sample 1) during the experiment A) 25 A, B) 50 A, C) 75 A, D) 100 A, E) 150 A, F) 200 A.

As shown in figure 3.2. We observe a higher heating rate for 100 A, 150 A, 200 A compared to the low heating rate observed for 25 A, 50 A, 75 A.
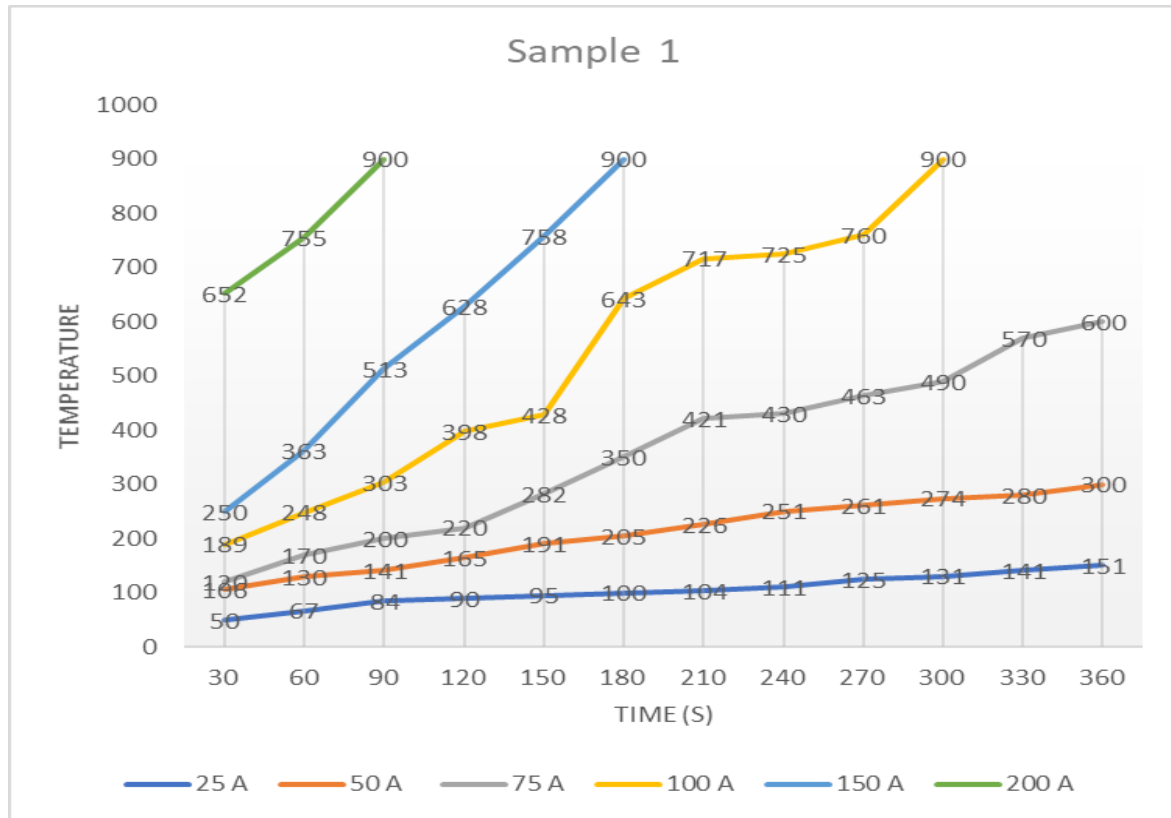
Figure 3.2. sample 1 heating curve.

3.2.2. Sample 2

As shown in table 3.3, we measured the graphite temperature change for 6 minutes using 30 seconds intervals at 25 A, 50 A, 75 A, 100 A, 150 A and 200 A. We can clearly observe the increase of the temperature with the increase of the time and current density.

At 50 A, the graphite sample exceeded the thermometer temperature limit after 330 seconds. The same thing was observed at 75 A after 270 seconds.

At 100 A the graphite sample exploded due to the excessive current density after 150 seconds, the same thing was observed at 150 A after 120 seconds and 200 A after 60 seconds.

Time (s)	25 A	50 A	75 A	100 A	150 A	200 A
30	124	245	236	420	425	515
60	188	267	345	593	696	900
90	220	294	400	745	761	/
120	272	322	571	770	900	/
150	294	344	674	900	/	/
180	430	387	696	/	/	/
210	455	425	710	/	/	/
240	509	510	777	/	/	/
270	514	687	900	/	/	/
300	530	750	/	/	/	/
330	590	900	/	/	/	/
360	677	/	/	/	/	/

Table 3.3. representation of the data (sample 2).

Figure 3.3. shows the heated graphite (sample 2) during our experiment at different current densities, the higher increase in graphite brightness is related to the increase in graphite temperature.
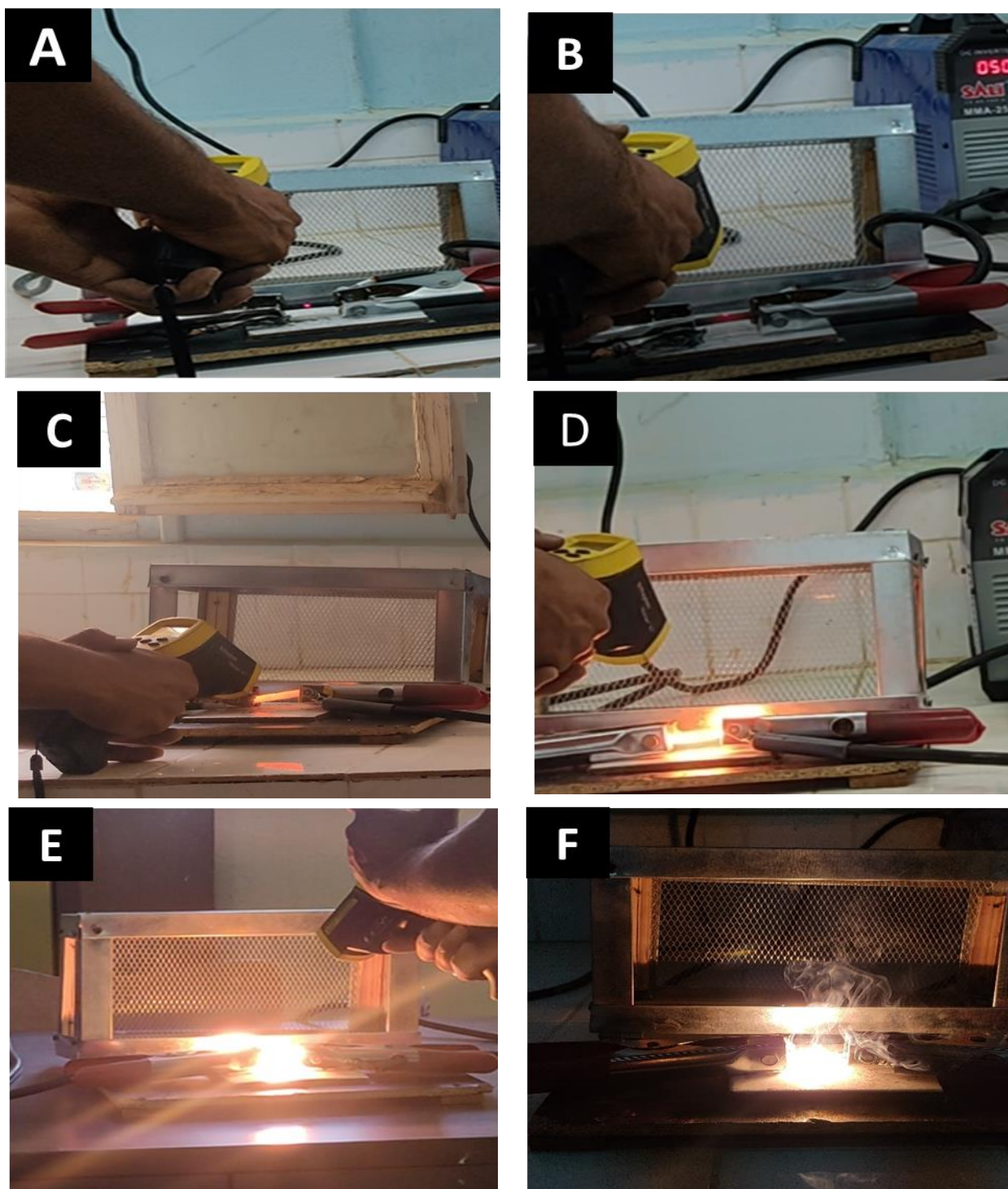
Figure 3.3. heated graphite (sample 2) during the experiment A) 25 A, B) 50 A, C) 75 A, D) 100 A, E) 150 A, F) 200 A.

As shown in Figure 3.4. We reached height temperature compared to sample 1 due to the smaller dimension.
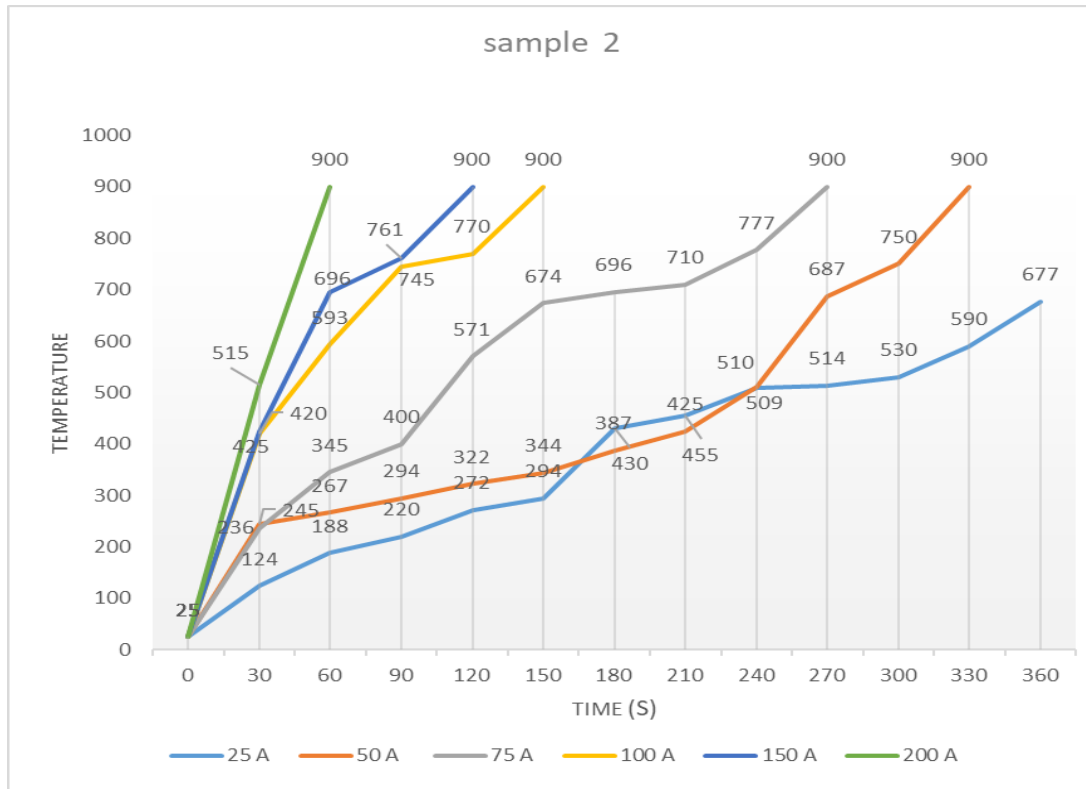
Figure 3.4. sample 2 heating curves

3.3.3. Sample 3

As shown in Table 3.4. We measured the graphite temperature change for 6 minutes using 30 seconds intervals at 25 A, 50 A, 75 A, 100 A, 150 A, and 200 A. We can clearly observe the increase of the temperature with the increase of time and current density.

At 25 A, the graphite sample reached 557 °C after 210 s, and then the temperature gradually decreased to 319 ° C after 360 seconds.

At 50 A, the graphite sample exceeded the thermometer temperature limit after 150 seconds.

At 75 A the graphite sample exploded due to the excessive current density after 150 seconds, the same thing was observed at 100 A after 60 seconds, 150 A, and 200 A after less than 30 seconds.

Time (s)	25 A	50 A	75 A	100 A	150 A	200 A
30	184	254	367	720	/	/
60	274	394	464	900	/	/
90	300	564	653	/	/	/
120	327	744	754	/	/	/
150	420	900	900	/	/	/
180	541	/	/	/	/	/
210	557	/	/	/	/	/
240	357	/	/	/	/	/
270	334	/	/	/	/	/
300	330	/	/	/	/	/
330	322	/	/	/	/	/
360	319	/	/	/	/	/

Table 3.4. representation of the data for (sample 3).

Figure 3.5. Shows the heated graphite (sample 3) during our experiment at different current densities, the higher increase in graphite brightness is related to the increase in graphite temperature.
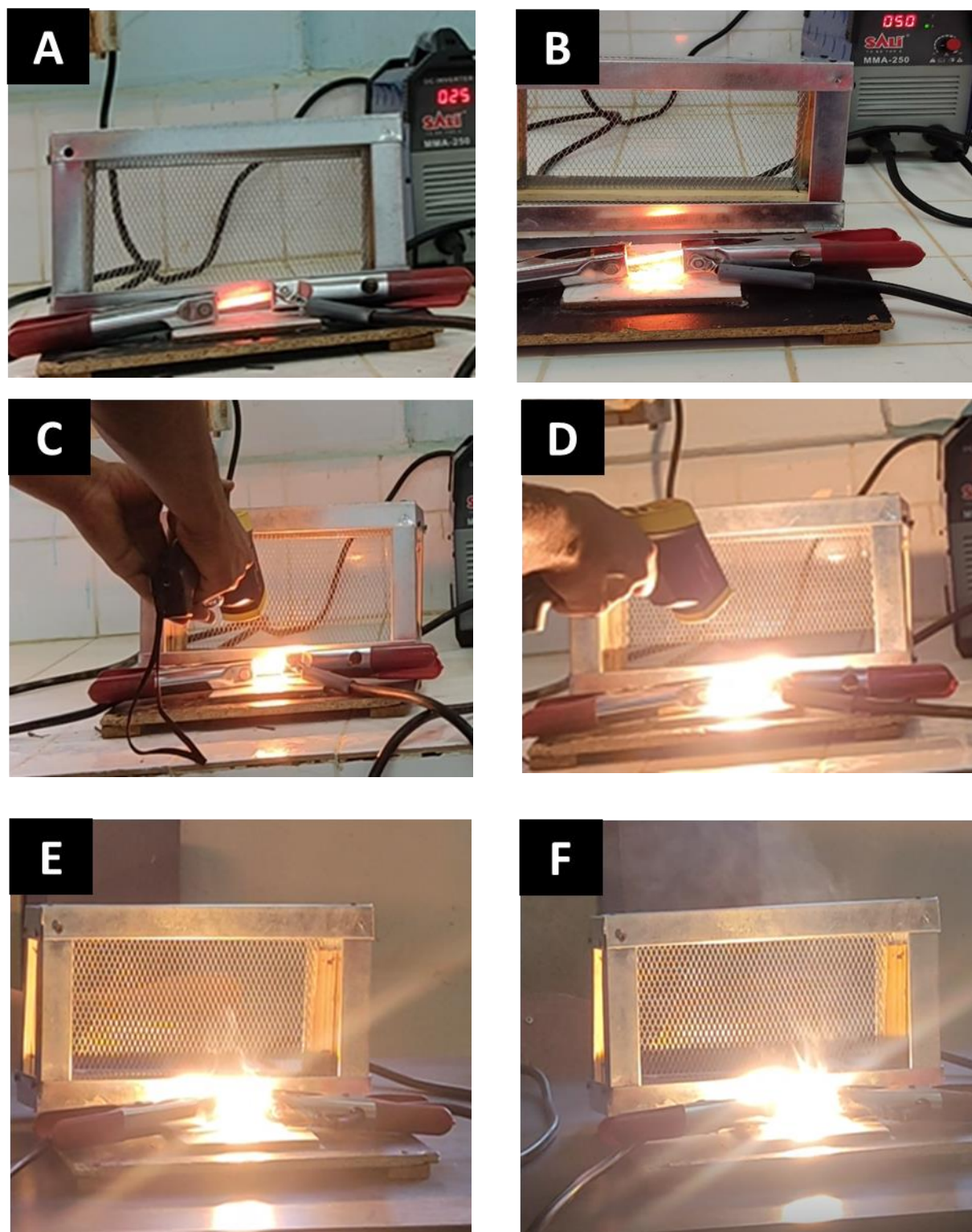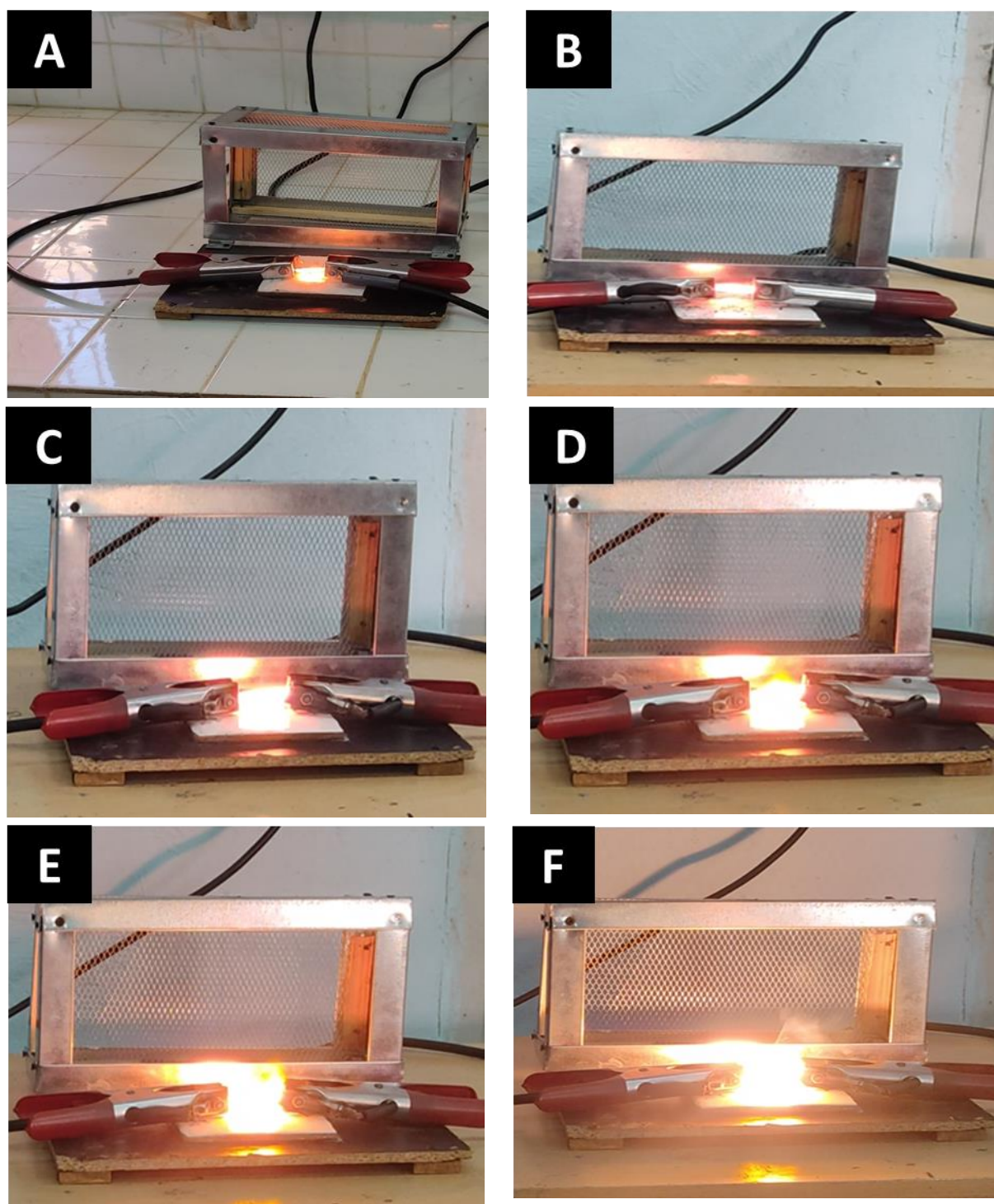
Figure 3.5. heated graphite (sample 3) during the experiment A) 25 A, B) 50 A, C) 75 A, D) 100 A, E) 150 A, F) 200 A.

As shown in Figure 3.6. graphite has lost electrical properties due to high heating at 25 A. We observe a higher heating rate for 50 A,75 A, 100 A. and, we reached height temperature at 150 A, 200 A after less than 30 seconds.
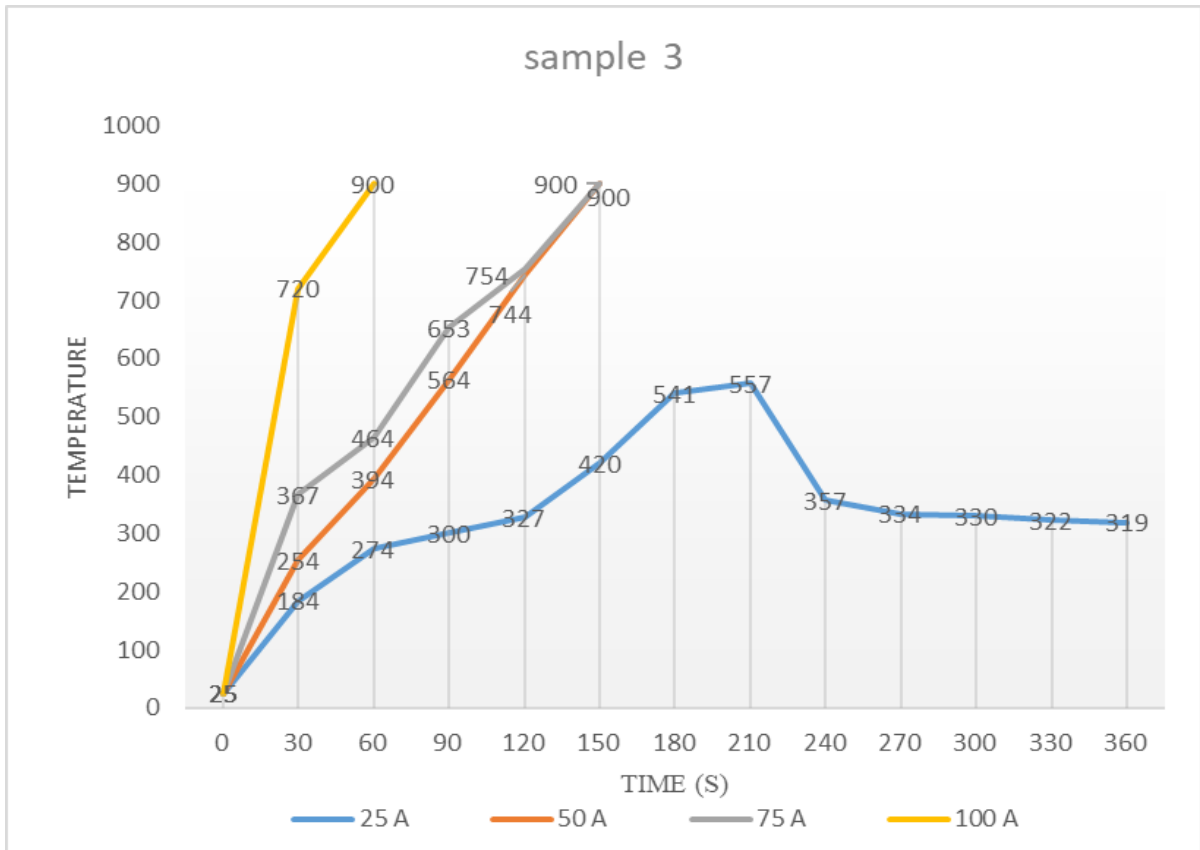
Figure 3.6. sample 3 heating curves

3.4. Sintering experimental

3.4.1. Sample 1: Aluminum powder

In this experiment, we pressed aluminum powder into the graphite die as shown in figure 3.7, then we connect the graphite die to the DC generator.

Figure 3.7. Aluminum powder pressed into a graphite die.

In this experiment, after the graphite die was connected to the DC generator, the temperature reached 145 °C at 25(A) 2 minutes after the start of the experiment. We observe that the temperature of the aluminum sample increases with the increase of the current density, and we set it to 100 (A) for 1 min. The aluminum sample exceeded the temperature limit of the thermometer. Then we decrease the current density to 25 (A) gradually. Figure 3.8. Shows the sintering curve of the aluminum sample.

Figure 3.8. The sintering curve for the aluminum sample.

As shown in figure 3.9A, we couldn't extract the sintered Aluminum sample without destroying the graphite Die because the sintered sample was partially diffused in the graphite, we observed that the sintered sample is divided into 3 different solid parts of non-uniform shapes. After minor polishing, we obtained the solid sample shown in figure 3.9B, a rough surface and the presence of small pores could be easily observed. The absence of the applied pressure during the sintering process and the excessive sintering temperature are the reasons of the non-homogeneous shapes and separated sintered samples.

Figure 3.9. Sintered aluminum powder (sample 1).

3.4.2. Sample 2: Copper powder

In this experiment, we pressed copper powder into the graphite die, then we connect the graphite die to the DC generator as shown in figure 3.10.

Figure 3.10. Copper powder pressed into a graphite die.

In this experiment, after the graphite die was connected to the DC generator, the temperature reached 158 °C at 25(A) 2 minutes after the start of the experiment. We observe the temperature of the copper sample increases with the increase of the current density, in the first experiment we set it to 150 (A) for 4 minutes, it was clearly observed the copper sample exceeded the melting temperature as shown in Figure. 3.11. In the second experiment, we set it to 150 (A) for 1 minute, the copper sample exceeded the temperature limit of the thermometer. Then we decrease the current density to 25 A gradually. Figure 3.12. Shows the sintering curve of the copper sample.
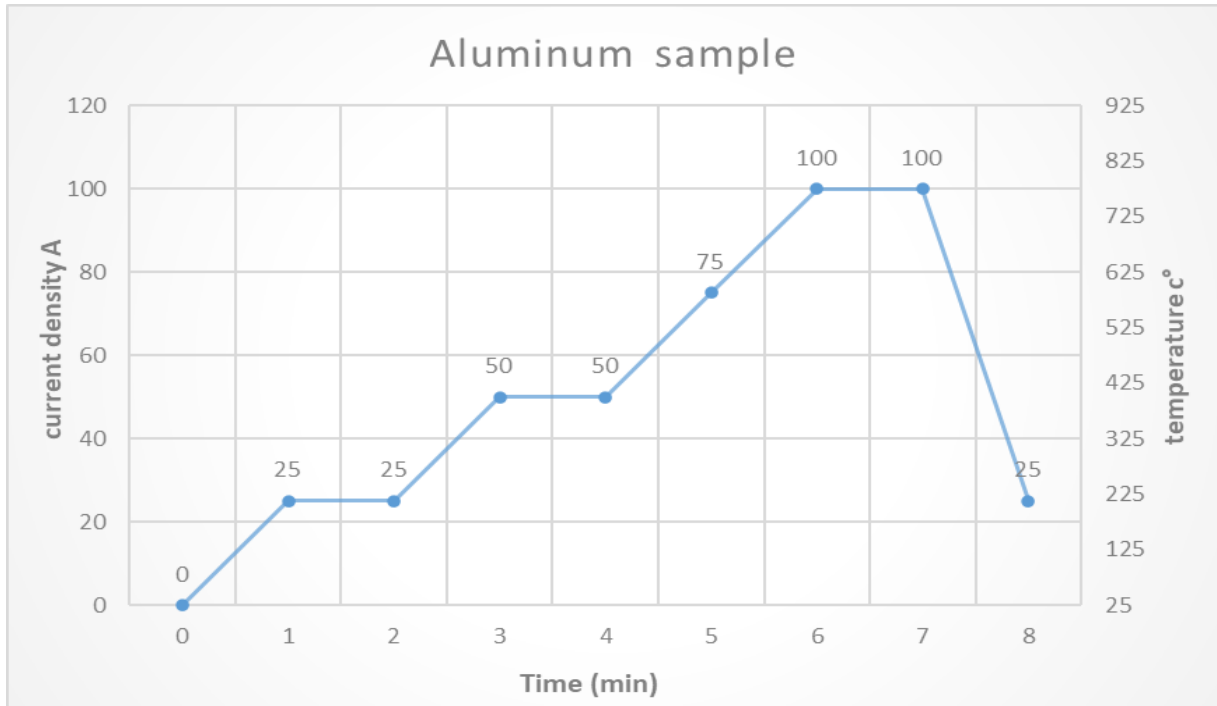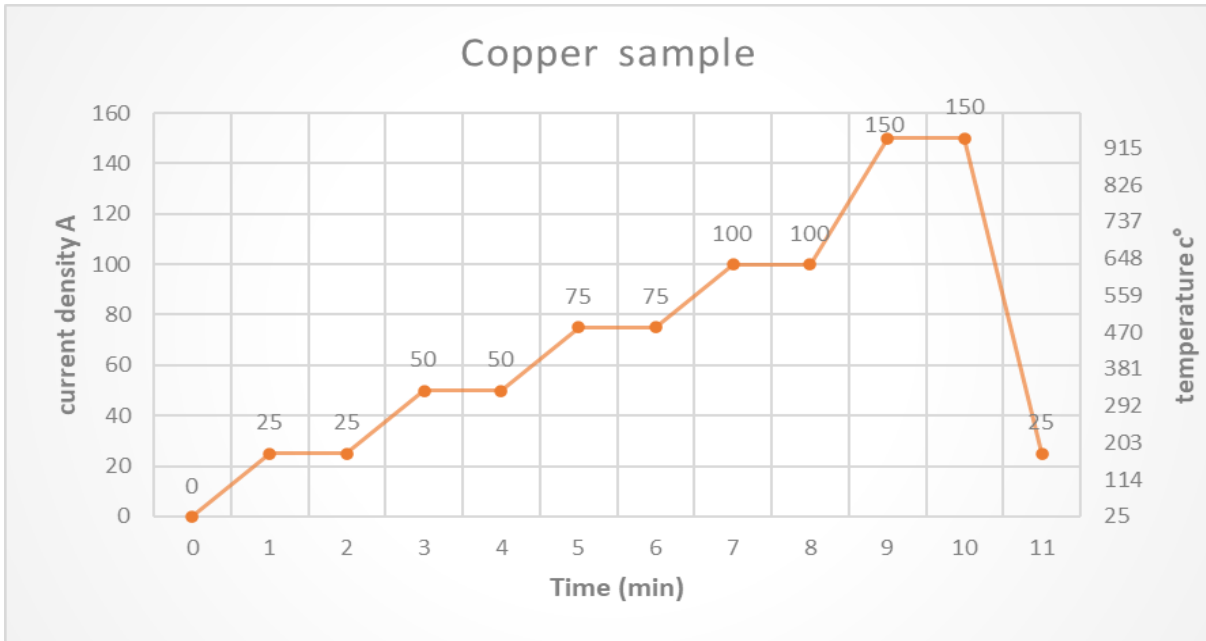
Figure 3.11. The sintering curve for the copper sample.

Figure 3.12. The first experiment when the copper sample exceeded the melting temperature.

As shown in figure 3.13A, we couldn't extract the sintered copper sample without destroying the graphite Die because the sintered sample was partially diffused in the graphite, after minor polishing, we obtained the solid sample shown in figure 3.13B, a rough surface and the presence of small pores could be easily observed. The absence of the applied pressure during the sintering process and the excessive sintering temperature are the reasons for the non-homogeneous shapes and separated sintered samples.
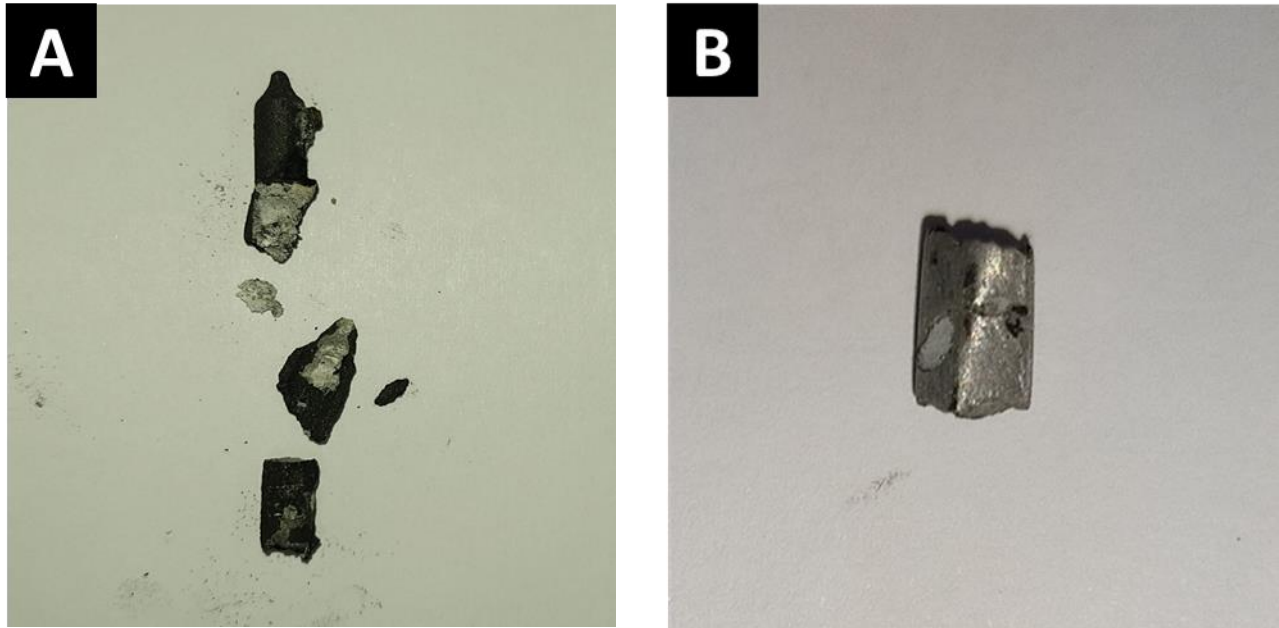
Figure 3.13. sintered copper powder (sample 2).

3.4.3. Sample 3: Iron powder

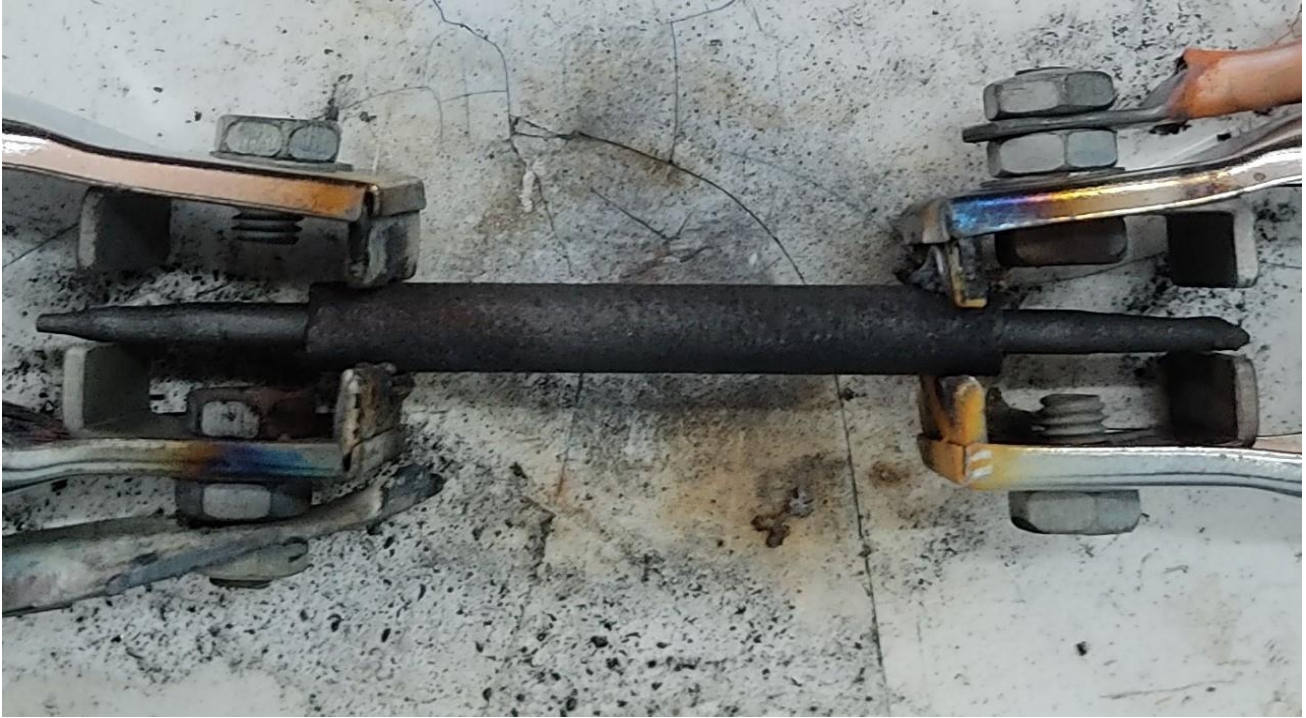In this experiment, we pressed iron powder into the graphite die as shown in figure 3.14.

Figure 3.14. Iron powder pressed into a graphite die.

In this experiment, after the graphite die was connected to the DC generator, the temperature reached 140 °C at 50 (A) 3 minutes after the start of the experiment. We observe that the temperature of the iron sample increases with the increase of the current density, and we set it to 150 (A) for 2 min then we increase the current density to 200 (A) for 1 min. The iron sample exceeded the temperature limit of the thermometer. Then we decrease the current density to 25 (A) gradually. Figure 3.15. Shows the sintering curve of the iron sample.
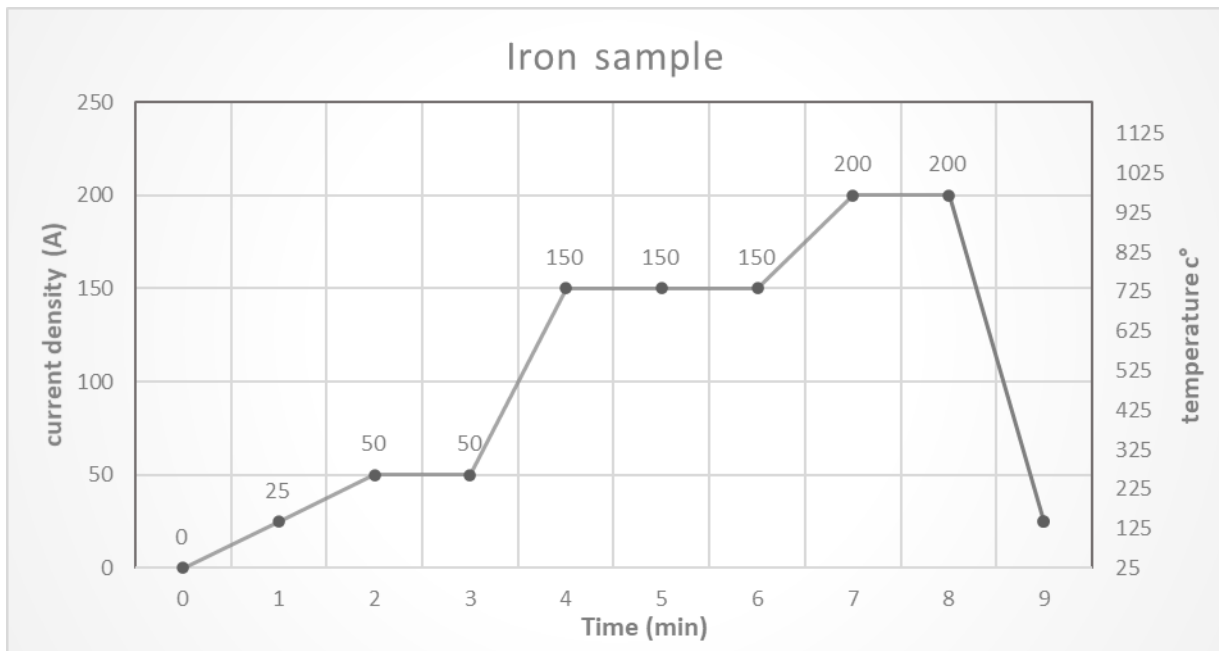
Figure 3.15. The sintering curve for the copper sample.

As shown in figure 3.16A, we couldn't extract the sintered iron sample without destroying the graphite Die because the sintered sample was partially diffused in the graphite, after minor polishing, we obtained the solid sample shown in figure 3.16B, a rough surface and the presence of small pores could be easily observed. The absence of the applied pressure during the sintering process and the excessive sintering temperature are the reasons for the non-homogeneous shapes and separated sintered samples.

Figure 3.16. sintered iron powder (sample 3).

General Conclusion

The result of our experiment shows the possibility of manufacturing mini spark plasma sintering using a small DC generator, the spark plasma sintering was successful for the three tested metal powders (aluminum, copper, and iron).

Even though we didn't apply any pressure during the spark plasma sintering, we could elaborate solid and compacted materials. Further investigations and experiments are needed in order to select the optimum parameters for the mini-spark plasma sintering Process.

Future work

Many different adaptations, tests, and experiments have been left for the future due to lack of equipment and materials (for example, the lack of noble graphite and Equipment needed in the experiment such as a proper thermocouple).

In the future (after mastering the sintering parameters of the mini-SPS) it would be interesting to focus on the elaboration of novel materials/composites and compare the obtained results with the published results of similar composites elaborated by available/ regular SPS process for efficiency and reliability aspect.

List of References

[1] MEZIANI, Hakima. Elaboration d'un composite WC/Cu par infiltration (Doctoral dissertation, Université de Tizi Ouzou-Mouloud Mammeri). (2013).

[2] Popovich, et al. Metal Powder Additive Manufacturing. New Trends in 3D Printing.

[3] Francis, L. F. Powder Processes. Materials Processing, (2016). 343–414.

[4] Kennard, F., Cold isostatic pressing. In: Schneider Jr., S.J. (Ed.), Engineered Materials Handbook, Vol. 4: Ceramics and Glasses. ASM International, Materials Park, 1991. OH, pp. 147-152.

[5] Oberacker, R. Powder compaction by dry pressing. Ceramics Science and Technology, (2012)., 3, 3-37.

[6] The Open University., (2017,11 December). cold-isostatic-pressing. Openlearn. [https://www.open.edu/openlearn/science-maths-technology/engineering-technology/manupedia/cold-isostatic-pressing].

[7] Mazor, et al. A combined DEM & FEM approach for modelling roll compaction process. Powder Technology, (2018). 337, 3-16.

[8] Akseli, t al. A Quantitative Correlation of the Effect of Density Distributions in Roller-Compacted Ribbons on the Mechanical Properties of Tablets Using Ultrasonics and X-ray Tomography. AAPS PharmSciTech, (2011). 12(3), 834–853.

[9] German, R. M. Sintering with External Pressure. Sintering: From Empirical Observations to Scientific Principles, (2014). 305–354.

[10] Dobrzanski, et al. Fabrication Technologies of the Sintered Materials Including Materials for Medical and Dental Application. Powder Metallurgy - Fundamentals and Case Studies. (2017).

[11] McNamara, et al. Powder Metallurgical Processing of NiTi Using Spark Plasma Sintering. Comprehensive Materials Finishing, (2017). 21(3), 336–346.

[12] Samal, et al. Powder metallurgy methods and applications. ASM handbook of powder metallurgy, (2015). 7.

[13] The Open University., (2017,11 December). Extrusion of Powders. Openlearn.

[https://www.open.edu/openlearn/science-maths-technology/engineering-technology/manupedia/extrusion-powders].

LIST OF REFERENCE

[14] Cavaliere, et al. Spark Plasma Sintering: Process Fundamentals. Spark Plasma Sintering of Materials, (2019). 3–20.

[15] Santanach, et al. Spark plasma sintering of alumina: Study of parameters, formal sintering analysis and hypotheses on the mechanism(s) involved in densification and grain growth. Acta Materialia, (2011). 59(4), 1400–1408.

[16] Nishiyabu, Powder space holder metal injection molding (PSH-MIM) of micro-porous metals. Handbook of Metal Injection Molding. (2012). 349–390.

[17] Todd, et al. Developments in metal injection molding (MIM). Advances in Powder Metallurgy, (2013). 109–146.

[18] Orrù, et al. Consolidation/synthesis of materials by electric current activated/assisted sintering. Materials Science and Engineering: R: Reports, (2009). 63(4-6), 127–287

[19] Grasso, et al. Electric current activated/assisted sintering (ECAS): a review of patents 1906–2008. Science and Technology of Advanced Materials, (2009). 10(5), 053001.

[20] Anselmi-Tamburini, U. Spark Plasma Sintering. Reference Module in Materials Science and Materials Engineering. (2019).

[21] Olevsky, et al. Field-assisted sintering. Science and Applications. (2018).

[22] Guillon, et al. Field-Assisted Sintering Technology/Spark Plasma Sintering: Mechanisms, Materials, and Technology Developments. Advanced Engineering Materials, (2014). 16(7), 830–849.

[23] Munir, et al. Electric Current Activation of Sintering: A Review of the Pulsed Electric Current Sintering Process. Journal of the American Ceramic Society, (2010). 94(1), 1–19.

[24] M. Suárez, et al. Challenges and opportunities for spark plasma sintering: a key technology for a new generation of materials. Sintering applications, (2013). 13, 319-342.

[25] Sharma, et al. Fundamentals of Spark Plasma Sintering (SPS): An Ideal Processing Technique for Fabrication of Metal Matrix Nanocomposites. Spark Plasma Sintering of Materials, (2019). 21–59.

[26] Yamazaki, et al. PAS (Plasma activated sintering): Transient sintering process control for rapid consolidation of powders. Journal of Materials Processing Technology, (1996). 56(1-4), 955–965.

[27] Clemares IA, et al. Transparent alumina/ceria nanocomposites by spark plasma sintering. Adv Eng. Mater. (2010). 12(11):1154–1160.

[28] Lukianova, et al. Microstructure of spark plasma-sintered silicon nitride ceramics. Nanoscale Res Lett, (2017). 12:293–299.

[29] Inoue K. Electric Discharge Heat Treatment of Metals in Electrolytes. US Patent No. (1965). 3,188,245, June

[30] Yanagisawa et al., Recent research on spark sintering. Materia Japan, (1994). 33, 12, 1489-1496.

[31] Groza, et al. Surface oxide debonding in field assisted powder sintering. Materials Science and Engineering A, (1999). 270, 2, 278-282

[32] Groza, et al. Sintering activation by external electrical field. Materials Science and Engineering. (2000)., 287, 2, 171-177.

[33] Tiwari, et al. Simulation of thermal and electrical field evolution during spark plasma sintering. Ceramics International, (2009). 35, 2, 699-708.

[34] Conrad, H. Thermally activated plastic flow of metals and ceramics with an electric field or current. Mater Sci Eng. (2002). A 322(1–2):100–107.

[35] Olevsky EA, et al. Consolidation enhancement in spark plasma sintering: impact of high heating rates. (2007). J Appl Phys 102(11):114913.

[36] Olevsky, EA, Froyen, L. Impact of thermal diffusion on densification during SPS. (2008). J Am Ceram Soc 92:122–132**.**

[37] Dmitri, Kopeliovich. (2012,06 January). Spark plasma sintering. Substech. [https://www.substech.com/dokuwiki/doku.php?id=spark_plasma_sintering].

[38] Demetrius T Paris., Frank Kenneth Hurd., Basic electromagnetic theory, McGraw-Hill, 591 p., p. 546.

[39] Andrew, et al. Clinical Electrophysiology: Electrotherapy and Electrophysiologic Testing (3rd ed.). Lippincott Williams & Wilkins. (2007). p. 10.

[40] Bhargava, et al. Basic Electronics & Linear Circuits. Tata McGraw-Hill Education. (1984). p. 90.

[41] Britannica, T. Editors of Encyclopedia (2019, May 2). Transformer. Encyclopedia Britannica.

[https://www.britannica.com/technology/transformer-electronics].

<div dir="rtl">

نبذة مختصرة

الهدف من هذه المذكرة هو دراسة إمكانية تصنيع SPS المصغرة بأقل تكلفة ممكنة.

تظهر نتيجة تجربتنا إمكانية تصنيع تلبيد بالشرارة المصغرة باستخدام مولد صغير للتيار المستمر ، وقد نجح تلبيد شرارة البلازما للمساحيق المعدنية الثلاثة المختبرة (الألمنيوم والنحاس والحديد).

على الرغم من أننا لم نطبق أي ضغط أثناء تلبيد شرارة البلازما ، يمكننا تطوير مواد صلبة ومضغوطة. هناك حاجة إلى مزيد من التحقيقات والتجارب من أجل تحديد المعلمات المثلى لعملية تلبيد البلازما بالشرارة الصغيرة.

</div>

Abstract

The objective of this note is to study the possibility of manufacturing mini SPS at the lowest possible cost.

The result of our experiment shows the possibility of manufacturing mini spark plasma sintering using a small DC generator, the spark plasma sintering was successful for the three tested metal powders (aluminum, copper, and iron).

Even though we didn't apply any pressure during the spark plasma sintering, we could elaborate solid and compacted materials. Further investigations and experiments are needed in order to select the optimum parameters for the mini-spark plasma sintering Process.

Résumé

L'objectif de cette note est d'étudier la possibilité de fabriquer des mini SPS au moindre coût possible.

Le résultat de notre expérience montre la possibilité de fabriquer des mini frittage plasma spark en utilisant un petit générateur de courant continu, le frittage plasma spark a été réussi pour les trois poudres métalliques testées (aluminium, cuivre et fer).

Même si nous n'avons appliqué aucune pression lors du frittage plasma par étincelle, nous avons pu élaborer des matériaux solides et compactés. D'autres investigations et expériences sont nécessaires afin de sélectionner les paramètres optimaux pour le procédé de frittage plasma à mini-étincelles.